Bulletin of Mathematical Biology (2022) 84:112
https://doi.org/10.1007/s11538-022-01054-y

Society for Mathematical Biology

ORIGINAL ARTICLE

A Mathematical Study of the Role of tBregs in Breast Cancer

Vasiliki Bitsouni[1,2] · **Nikolaos Gialelis**[1,3] · **Vasilis Tsilidis**[2]

Received: 3 March 2022 / Accepted: 12 July 2022 / Published online: 1 September 2022

Abstract
A model for the mathematical study of immune response to breast cancer is proposed and studied, both analytically and numerically. It is a simplification of a complex one, recently introduced by two of the present authors. It serves for a compact study of the dynamical role in cancer promotion of a relatively recently described subgroup of regulatory B cells, which are evoked by the tumour.

Keywords Cancer immunology · Tumour-evoked regulatory B cell · Mathematical modelling · Stability analysis · Bifurcation analysis · Numerical simulation

Mathematics Subject Classification 34A34 · 37G10 · 37M05 · 37N25 · 92B05 · 92D25 · 93A30

1 Introduction

The immune system, divided into the major components of innate and adaptive immunity, grants an organism the ability to detect invading pathogens and transformed cells (e.g. cancer cells)—namely differentiate between "self" and "non-self"—and to eliminate them. The provided type and measure of inflammation fit the circumstances, i.e.

Vasiliki Bitsouni, Nikolaos Gialelis and Vasilis Tsilidis have contributed equally to this work.

✉ Vasiliki Bitsouni
vbitsouni@math.uoa.gr

Nikolaos Gialelis
ngialelis@math.uoa.gr

Vasilis Tsilidis
vtsilidis@outlook.com

1 Department of Mathematics, National and Kapodistrian University of Athens, Panepistimioupolis, 15784 Athens, Greece

2 School of Science and Technology, Hellenic Open University, 18 Parodos Aristotelous Str., 26335 Patras, Greece

3 School of Medicine, National and Kapodistrian University of Athens, 115275 Athens, Greece

the immune system dynamically adjusts the induced inflammatory response (Segel and Cohen 2001). The latter function of the immune system is called *immune regulation*. The suppressing mechanisms for immune regulation act as a double-edged sword: on the one hand, they prevent from autoimmune diseases, but on the other hand, they inhibit immune response against cancer (Narendra et al. 2013). Indeed, it is currently accepted that an aberrant innate and adaptive immune response contributes to tumorigenesis by selecting aggressive clones, inducing immunosuppression, and stimulating cancer cell proliferation and metastasis (Gonzalez et al. 2018).

The immune system primarily consists of certain types of white blood cells, called lymphocytes. Innate immunity includes lymphocytes such as natural killer (NK) cells, while adaptive immunity includes T and B lymphocytes. Immune regulation involves a special subset of T cells, called regulatory T cells (Tregs) (Chraa et al. 2019). B cells also play a part in immune regulation in the form of regulatory B cells (Bregs) (Rosser and Mauri 2015). Even though the research on Cancer Immunology has been mainly concentrated on Tregs and NK cells, recently there has been an upsurge in research on Bregs associated with tumours (see e.g. Guo and Cui 2019 and the references therein).

In this work, we focus on *breast cancer* and we study the role of a relatively recently described (Olkhanud et al. 2009, 2011) subgroup of Bregs, the *tumour-evoked Bregs* (*tBregs*), in the immune response to the aforementioned type of cancer. *Breast cancer* is more than a hundred times more likely to affect a woman than a man (Fentiman et al. 2006), and it is the most common cause of cancer-related death in women world-wide (Bray et al. 2018; Ferlay et al. 2019). It is estimated that one in eight women living in the USA will develop breast cancer in her lifetime (Carol et al. 2014). *tBregs* protect metastasizing breast cancer cells from immune effector cells by inducing immune suppression mediated by Tregs (Biragyn et al. 2014). In a few words, breast cancer seems to generate tBregs, which in turn increase the proliferation of Tregs, which are responsible for the death of the tumour-lysing NK cells, leading eventually to lung metastasis (Olkhanud et al. 2011).

Our study is based on a *dynamical system of non-linear ordinary differential equations*. The theory of ordinary differential equations and dynamical systems has been deployed by scientists in order to gain new insights about the complex interactions between cancer and the immune system. To this end, several models have been constructed for the study of different entities concerning cancer–immune interactions such as cancer cells, normal cells, cytolytic cells, regulatory cells, cytokines, cancer cells at different stages as well as various therapies (Kuznetsov et al. 1994; Nani and Freedman 2000; Pillis and Radunskaya 2003; Villasana and Radunskaya 2003; Byrne et al. 2004; Khailaie et al. 2013; López et al. 2014; den Breems and Eftimie 2016; Al-Tuwairqi and Al-Johani 2020; Senekal et al. 2021).

The proposed model is a *simplification* of a complex one recently introduced in Bitsouni and Tsilidis (2022). In general, the complexity of the models appeared in bibliography vary greatly. On the one hand, lower-dimensional and with simpler functional responses models are advantageous in that they allow for the straightforward application of mathematical techniques, including those of stability and bifurcation analysis (Szymańska 2003; Bunimovich-Mendrazitsky et al. 2007; Phan and Tian 2017; Ghosh and Banerjee 2018). However, their low dimension inhibits the simultaneous investigation of more complex mechanisms that involve multiple components

of the tumour micro-environment. On the other hand, higher-dimensional models with complex functional responses are more realistic (de Pillis et al. 2009, 2013; He and Xu 2017; Makhlouf et al. 2020). However, they are much more difficult to analyse and can mainly be studied through numerical methods. Nevertheless, both approaches have led to significant insights into the biological mechanisms governing tumour–immune system interactions (Eftimie et al. 2011).

The present study is organised as follows: In Sect. 2, we construct the mathematical model governing the interactions between breast cancer cells, NK cells, Tregs and tBregs, for which we prove some basic properties of its solution, necessary for ensuring the model's biological relevance, in Appendix A. In Sect. 3, we conduct local stability analysis using the linearisation theorem, as well as the center manifold theorem for the cases in which our equilibrium points are non-hyperbolic. In Sect. 4, we investigate the local bifurcations of our model. In Sect. 5, we perform numerical simulations in order to confirm our qualitative results and further analyse our model. Finally, in Sect. 6, we sum up and review our results.

2 Model Formulation

In this section, we develop a relatively simple mathematical model in an attempt to study the interactions between breast cancer cells, NK cells, Tregs and tBregs.

Such a model is a simplification of a complex one, recently introduced in Bitsouni and Tsilidis (2022), where seven types of interacting cells are considered, i.e. breast cancer cells, NK cells, Tregs and tBregs, $CD8^+$ T cells, non-Treg $CD4^+$ T cells, non-Treg $CD4^+$ T cells and non-tBreg B cells. A schematic representation of the interactions between these seven types of cells is given in Fig. 1.

As a first step towards a simplified model of Bitsouni and Tsilidis (2022), we follow (Olkhanud et al. 2011) and we consider only the interactions between breast cancer cells, NK cells, Tregs and tBregs, which are now depicted in Fig. 2, omitting the rest of the interactions.

Hence, denoting the populations of those cells as T, N, R and B, respectively, and considering them as functions of time, t, measured in days, we deduce the following general system of coupled non-linear ordinary equations:

$$\begin{aligned}
\frac{\mathrm{d}T}{\mathrm{d}t} &= f_T(T) + f_{T,N}(T, N)\,,\\
\frac{\mathrm{d}N}{\mathrm{d}t} &= f_N(N) + f_{N,R}(N, R)\,,\\
\frac{\mathrm{d}R}{\mathrm{d}t} &= f_R(R) + f_{R,B}(R, B)\,,\\
\frac{\mathrm{d}B}{\mathrm{d}t} &= f_B(B) + f_{T,B}(T, B)\,,
\end{aligned}$$

where f_T, f_N, f_R and f_B stand for the rates of the corresponding cell populations in the absence of interactions, and on the other hand, $f_{T,N}$, $f_{N,R}$, $f_{R,B}$ and $f_{T,B}$ stand for the additional rates in the presence of interactions.

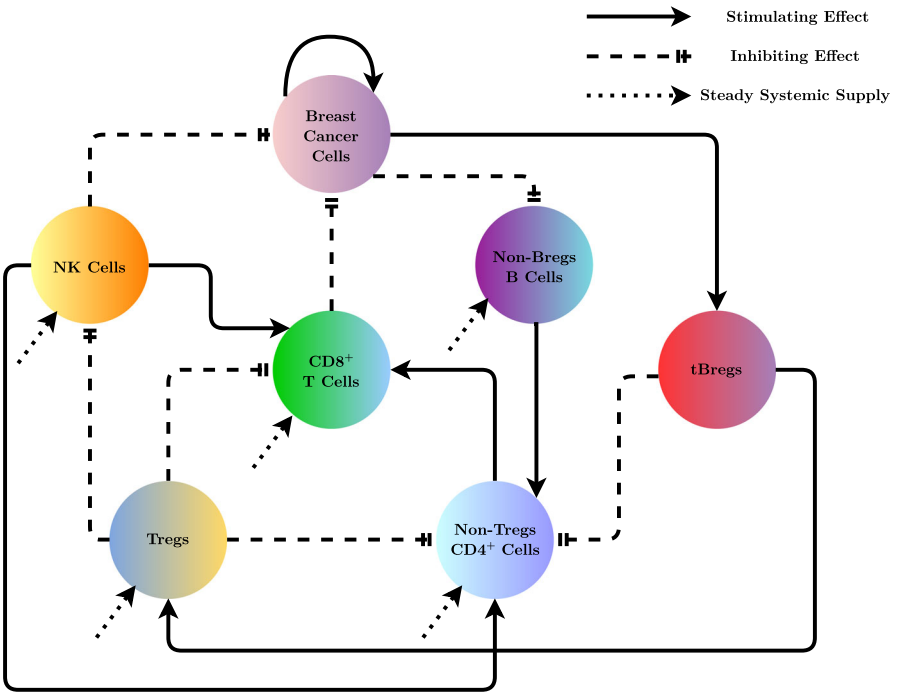

Fig. 1 Interactions between the cells in the model described in Bitsouni and Tsilidis (2022). Solid line (—): Stimulating effect. Dashed line (- -): Inhibiting effect. Dotted line (· · ·): Steady systemic supply. Figure adapted from Bitsouni and Tsilidis (2022), with the inclusion of the present, yet previously non-depicted, steady systemic supply (Color figure online)

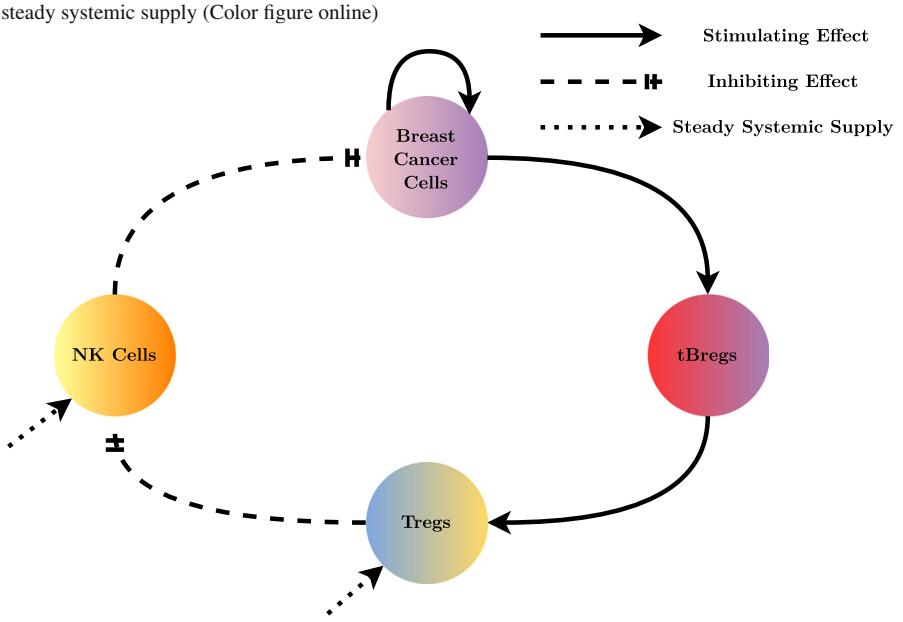

Fig. 2 Interactions between the cells in the simplified model. Solid line (—): Stimulating effect. Dashed line (- -): Inhibiting effect (Color figure online)

We then make the following assumptions:

1. We utilise the non-interaction terms of Bitsouni and Tsilidis (2022), i.e. we consider logistic growth for the breast cancer cell population, while exponential decay of the rest populations.
2. As far as the interaction terms are concerned:
   i. The Treg-induced NK cell inhibition coefficient parameter is eliminated. Besides, to the best of authors' knowledge, there are no data concerning its values in the bibliography. Moreover, the Hill function, which is used to model the NK-induced breast cancer cell lysis, is replaced by the simpler linear function. Besides, such a choice is followed in various other models to capture the same dynamics (see Bitsouni and Tsilidis 2022 and references therein).
   ii. We drop the interaction between breast cancer cells and NK cells, i.e. the NK death mechanism by exhaustion of tumour-killing resources. Besides, in Bitsouni and Tsilidis (2022) the value of the corresponding parameter is estimated to be small. Moreover, for the shake of simplicity, we consider linear function for the modelling of interaction between NK calls and Tregs.
   iii. As for the interaction term between Tregs and tBregs, in Bitsouni and Tsilidis (2022) a linear function was used, which involved an intermediate cell type—in particular, non-Treg $CD4^+$ T cells—that is omitted here. We consider the same functional response without the presence of any intermediate cell population.
   iv. The condition for the interaction between breast cancer cells and tBregs in Bitsouni and Tsilidis (2022) remains unchanged here.

   At the end of the day, the rate of every interaction between two cell populations is the product of the size of the two populations, i.e. we consider Holling's type I functional response for every interacting population.

To sum up, we get the following system of ordinary differential equations:

$$\frac{\mathrm{d}T}{\mathrm{d}t} = aT(1 - bT) - cNT\,, \tag{1a}$$

$$\frac{\mathrm{d}N}{\mathrm{d}t} = \sigma - \theta_N N - \gamma RN\,, \tag{1b}$$

$$\frac{\mathrm{d}R}{\mathrm{d}t} = \kappa - \theta_R R + m_B BR\,, \tag{1c}$$

$$\frac{\mathrm{d}B}{\mathrm{d}t} = -\theta_B B + m_T TB\,, \tag{1d}$$

for some positive constants a, b, c, σ, θ_N, γ, κ, θ_R, m_B, θ_B and m_T, along with the initial condition:

$$(T\,(0)\,,N\,(0)\,,R\,(0)\,,B\,(0)) = (T_0, N_0, R_0, B_0) \in \mathbb{R}^4_{\geq 0}. \tag{2}$$

Table 1 lists all the parameters of our model, along with a brief description about each one, as well as their units. We subsequently give an explanation about each term of our model.

Table 1 Description and units of the parameters of system (1)

Prm.	Description	Unit
a	Tumour growth rate	day^{-1}
b	Inverse of the tumour carrying capacity	cell^{-1}
c	Rate of NK-induced tumour death	$\text{cell}^{-1} \cdot \text{day}^{-1}$
σ	Constant source of NK cells	$\text{cell} \cdot \text{day}^{-1}$
θ_N	Rate of programmable NK cell death	day^{-1}
γ	Rate of NK cell death due to Tregs	$\text{cell}^{-1} \cdot \text{day}^{-1}$
κ	Constant source of Tregs	$\text{cell} \cdot \text{day}^{-1}$
θ_R	Rate of programmable Treg death	day^{-1}
m_B	Rate of tBreg-induced Treg activation	$\text{cell}^{-1} \cdot \text{day}^{-1}$
θ_B	Rate of programmable tBreg cell death	day^{-1}
m_T	Rate of breast-cancer-induced tBreg activation	$\text{cell}^{-1} \cdot \text{day}^{-1}$

The first term of the right-hand side of equation (1a) models the logistic growth of breast cancer cells, while the second term models the death of breast cancer cells due to NK cells. We can show that (see Proposition 15) the set $[0, 1/b]$ is positively invariant for the component T of the solution of initial value problem {(1), (2)} (from now on: IVP). Hence, by analogy with the terminology used for the logistic equation, we say that the (positive) constant $1/b$ is the *tumour carrying capacity* for IVP. It expresses a maximal reachable size due to competition between adjacent cells, e.g. for space or nutrients (Vaghi et al. 2020). In general, the metastatic potential of a tumour increases as it reaches its carrying capacity. The conventional linear correlation between primary tumour size and the likelihood of metastasis (to the lymph nodes or to distant sites) is questioned, as a characteristic non-linear relationship, with a sigmoid corresponding curve, has already been described (see e.g. Sopik and Narod 2018 and the references therein).

As far as equation (1b) is concerned, parameter σ models the steady source of NK cells. The second term models the natural death of NK cells, whereas the last term models the Treg-induced NK apoptosis.

Regarding equation (1c), much like equation (1b), parameter κ models the steady source of Tregs. The second term models the natural death of Tregs, whereas the last term models the proliferation of Tregs due to tBregs.

Finally, the first term of equation (1d) models the natural death of tBregs, whereas the last term models their proliferation due to the existence of breast cancer.

3 Equilibria and Stability Analysis

We continue our analysis by finding the equilibrium points of system (1), which we write as $E = \left(\overline{T}, \overline{N}, \overline{R}, \overline{B}\right)$. To do so, we equate the right-hand side of (1) to $\mathbf{0}$ and solve the resulting system of algebraic equations

$$a\overline{T}(1-b\overline{T}) - c\overline{N}\,\overline{T} = 0\,, \tag{3a}$$
$$\sigma - \theta_N\overline{N} - \gamma\overline{R}\,\overline{N} = 0\,, \tag{3b}$$
$$\kappa - \theta_R\overline{R} + m_B\overline{B}\,\overline{R} = 0\,, \tag{3c}$$
$$-\theta_B\overline{B} + m_T\overline{T}\,\overline{B} = 0\,. \tag{3d}$$

Proposition 1 *System (1) has three equilibrium points*

$$E_1 = \left(0, \frac{a}{c_1}, \frac{\kappa}{\theta_R}, 0\right),$$
$$E_2 = \left(\frac{c_1 - c}{bc_1}, \frac{a}{c_1}, \frac{\kappa}{\theta_R}, 0\right) \quad \textit{and}$$
$$E_3 = \left(\frac{\theta_B}{m_T}, -\frac{a\Theta_1}{cm_T}, -\frac{\Theta_2}{a\gamma\Theta_1}, \frac{\sigma m_T\theta_R\,(c-c_2)}{m_B\Theta_2}\right),$$

where

$$\Theta_1 := b\theta_B - m_T,$$
$$\Theta_2 := a\theta_N\Theta_1 + c\sigma m_T,$$
$$c_1 := \frac{a\,(\theta_N\theta_R + \gamma\kappa)}{\theta_R\sigma},$$
$$c_2 := -\frac{\Theta_1 c_1}{m_T},$$

for which we can easily see that $c_1 > c_2 = \left(1 - \frac{b\theta_B}{m_T}\right)c_1$.

Proof From equation (3a), we see that either $\overline{T} = 0$ or $a(1-b\overline{T}) - c\overline{N} = 0$. In the case where $\overline{T} = 0$, by replacing $\overline{T} = 0$ to equation (3d), we get that $\overline{B} = 0$, which we consequently replace to equation (3c) to get $\overline{R} = \kappa/\theta_R$. Replacing the derived value of $\overline{R}$ to equation (3b), we get that $\overline{N} = (\sigma\theta_R)/(\gamma\kappa + \theta_N\theta_R)$, which yields the equilibrium point E_1.

We next assume that $\overline{T} \neq 0$, thus $a(1-b\overline{T}) - c\overline{N} = 0$. From equation (3d), we see that either $\overline{B} = 0$ or $\overline{T} = \theta_B/m_T$. In the case where $\overline{B} = 0$, we follow the same procedure as in the above paragraph to find the values of $\overline{N}$ and $\overline{R}$, which are equal to their respective counterpart from equilibrium E_1. Then, by replacing $\overline{N}$ to equation $a(1-b\overline{T}) - c\overline{N} = 0$, we get $\overline{T} = (a\gamma\kappa + a\theta_N\theta_R - c\sigma\theta_R)/(ab\gamma\kappa + ab\theta_N\theta_R)$ which gives us the second equilibrium point, E_2.

Finally, we have the case where $\overline{T} \neq 0$ and $\overline{B} \neq 0$. From equation (3d), we see that $\overline{T} = \theta_B/m_T$. By replacing it to equation $a(1-b\overline{T}) - c\overline{N} = 0$, we find $\overline{N} = (a\,(m_T - b\theta_B))\,/\,(cm_T)$. Subsequently, replacing $\overline{N}$ to (3b), we get that $\overline{R} = (ab\theta_B\theta_N - a\theta_N m_T + c\sigma m_T)/(a\gamma\,(m_T - b\theta_B))$ and by replacing $\overline{R}$ to equation (3c), we find $\overline{B} = (a\,(m_T - b\theta_B)\,(\gamma\kappa + \theta_N\theta_R) - c\sigma m_T\theta_R)/(m_B\,(a\theta_N\,(m_T - b\theta_B) - c\sigma m_T))$, which gives us the third equilibrium point, E_3. □

Since we are only interested in the cases where our variables are non-negative, we determine the conditions under which the equilibrium points' coordinates are non-negative.

Proposition 2 *Admissible (i.e. with non-negative components) equilibrium point E_1 exists for any set of parameters.*

Proof It is evident that the coordinates of E_1 are non-negative since all the parameters are positive. □

Proposition 3 *Admissible equilibrium point E_2 exists when $c \leq c_1$. If $c = c_1$, then $E_1 \equiv E_2$ and if $c < c_1$, then $E_1 \neq E_2$.*

Proof In order for E_2 to have non-negative coordinates, the numerator of its first coordinate needs to be non-negative, thus $c_1 - c \geq 0$. However, if $c_1 - c = 0$, then the first coordinate of E_2 becomes zero, therefore $E_1 \equiv E_2$. Hence, E_2 exists and does not coincide with E_1 when $c < c_1$. □

Proposition 4 *Admissible equilibrium point E_3 exists when $c \geq c_2$ and $\frac{\theta_B}{m_T} < \frac{1}{b}$. If $c = c_2$, then $E_2 \equiv E_3$ and if $c > c_2$, then $E_2 \neq E_3$.*

Proof Clearly, the first coordinate of E_3 is positive. For its second coordinate to be non-negative, $\Theta_1 \leq 0$ must hold. However, when $\Theta_1 = 0$, the denominator of the third coordinate of E_3 becomes zero. Therefore, assuming that $\Theta_1 \neq 0$, we have that $\Theta_1 < 0$ or equivalently $\frac{\theta_B}{m_T} < \frac{1}{b}$.

Since $\Theta_1 < 0$, then the numerator of the third coordinate of E_3 needs to be non-negative, thus $\Theta_2 \geq 0$. However, if $\Theta_2 = 0$, then the denominator of the fourth coordinate of E_3 becomes zero. Therefore, assuming that $\Theta_2 \neq 0$, we have that $\Theta_2 > 0$ or equivalently $\frac{a\theta_N - c\sigma}{ab\theta_N} < \frac{\theta_B}{m_T}$.

Since we assumed that $\Theta_2 > 0$, for its forth coordinate to be non-negative, $c \geq c_2$ must hold or equivalently $\frac{a\gamma\kappa + a\theta_N\theta_R - c\sigma\theta_R}{ab\gamma\kappa + ab\theta_N\theta_R} \leq \frac{\theta_B}{m_T}$.

We need to determine which of the two lower bounds of $\frac{\theta_B}{m_T}$ we found is the greatest, so we can take that as our lower bound for $\frac{\theta_B}{m_T}$. Let $\frac{a\gamma\kappa + a\theta_N\theta_R - c\sigma\theta_R}{ab\gamma\kappa + ab\theta_N\theta_R} < \frac{a\theta_N - c\sigma}{ab\theta_N}$. It follows that

$$\frac{a\gamma\kappa + a\theta_N\theta_R - c\sigma\theta_R}{\gamma\kappa + \theta_N\theta_R} < \frac{a\theta_N - c\sigma}{\theta_N} \Leftrightarrow a - \frac{c\sigma\theta_R}{\gamma\kappa + \theta_N\theta_R} < a - \frac{c\sigma}{\theta_N} \Leftrightarrow \gamma\kappa < 0,$$

which is impossible, therefore we have that $\frac{a\gamma\kappa + a\theta_N\theta_R - c\sigma\theta_R}{ab\gamma\kappa + ab\theta_N\theta_R} \geq \frac{a\theta_N - c\sigma}{ab\theta_N}$ and we choose $\frac{a\gamma\kappa + a\theta_N\theta_R - c\sigma\theta_R}{ab\gamma\kappa + ab\theta_N\theta_R}$ as our lower bound for $\frac{\theta_B}{m_T}$.

However, when $\frac{a\gamma\kappa + a\theta_N\theta_R - c\sigma\theta_R}{ab\gamma\kappa + ab\theta_N\theta_R} = \frac{\theta_B}{m_T}$, we have that $E_2 \equiv E_3$. Therefore, when E_2 does not coincide with E_3, then $\frac{a\gamma\kappa + a\theta_N\theta_R - c\sigma\theta_R}{ab\gamma\kappa + ab\theta_N\theta_R} < \frac{\theta_B}{m_T}$, and the proposition is proved. □

We next study the local stability of system (1) using the linearisation theorem, as well as the center manifold theorem in the cases where the equilibrium point is non-hyperbolic, while also utilising Descartes' rule of signs in the case where the Jacobian matrix's eigenvalues are too complex to be computed.

We begin by computing the Jacobian matrix of system (1) to be equal to

$$\mathbf{J}(T,N,R,T) = \begin{bmatrix} a-2abT-cN & -cT & 0 & 0 \\ 0 & -\theta_N-\gamma R & -\gamma N & 0 \\ 0 & 0 & -\theta_R+m_B B & m_B R \\ m_T B & 0 & 0 & -\theta_B+m_T T \end{bmatrix}.$$

Proposition 5 *Equilibrium point E_1, when it does not coincide with E_2, is locally asymptotically stable (stable node) if $c > c_1$ and unstable (saddle) if $c < c_1$.*

Proof At the equilibrium point E_1, the Jacobian matrix becomes

$$\mathbf{J}(E_1;c) = \begin{bmatrix} \frac{a(c_1-c)}{c_1} & 0 & 0 & 0 \\ 0 & -\frac{\sigma c_1}{a} & -\frac{a\gamma}{c_1} & 0 \\ 0 & 0 & -\theta_R & \frac{\kappa m_B}{\theta_R} \\ 0 & 0 & 0 & -\theta_B \end{bmatrix}, \tag{4}$$

with corresponding eigenvalues

$$\lambda_{11}(c) = \frac{a(c_1-c)}{c_1},\ \lambda_{12} = -\theta_B,\ \lambda_{13} = -\theta_R \quad \text{and} \quad \lambda_{14} = -\frac{\sigma c_1}{a}. \tag{5}$$

It is clear that the eigenvalues $\lambda_{12}, \lambda_{13}$ and λ_{14} are always negative since all the parameters are positive, while $\lambda_{11}(c)$ is negative when $c > c_1$ and positive when $c < c_1$. □

Remark 1 Note that the corresponding eigenvectors of matrix (4) are

$$\mathbf{u}_{11} = \left[1,0,0,0\right]^{\mathsf{T}}, \quad \mathbf{u}_{12} = \left[0, -\frac{a^2\gamma\kappa m_B}{c_1\theta_R(\theta_B-\theta_R)(a\theta_B-\sigma c_1)}, -\frac{\kappa m_B}{\theta_R(\theta_B-\theta_R)}, 1\right]^{\mathsf{T}}, \tag{6}$$

$$\mathbf{u}_{13} = \left[0, \frac{a^2\gamma}{c_1(a\theta_R-\sigma c_1)}, 1, 0\right]^{\mathsf{T}} \quad \text{and} \quad \mathbf{u}_{14} = \left[0,1,0,0\right]^{\mathsf{T}}. \tag{7}$$

In the case where λ_{11} is positive, we have that the local stable invariant manifold is tangent to the stable manifold of the linearised system, which is $E^s = \text{span}\{\mathbf{u}_{12}, \mathbf{u}_{13}, \mathbf{u}_{14}\}$, while the local unstable invariant manifold is tangent to the unstable manifold of the linearised system, which is $E^u = \text{span}\{\mathbf{u}_{11}\}$, that is the T axis. Biologically, this means that a small initial number of tumour cells will increase even with the presence of normal levels of NK cells, Tregs and tBregs.

Proposition 6 *Admissible equilibrium point E_2, when it does not coincide with E_3, is locally asymptotically stable (stable node) if $c > c_2$ and unstable (saddle) if $c < c_2$.*

Proof At the equilibrium point E_2, the Jacobian matrix becomes

$$\mathbf{J}(E_2;c) = \begin{bmatrix} -\frac{a(c_1-c)}{c_1} & -\frac{c(c_1-c)}{bc_1} & 0 & 0 \\ 0 & -\frac{\sigma c_1}{a} & -\frac{a\gamma}{c_1} & 0 \\ 0 & 0 & -\theta_R & \frac{\kappa m_B}{\theta_R} \\ 0 & 0 & 0 & \frac{m_T(c_2-c)}{bc_1} \end{bmatrix},$$

with corresponding eigenvalues

$$\lambda_{21}(c) = \frac{m_T(c_2 - c)}{bc_1}, \ \lambda_{22} = -\theta_R, \ \lambda_{23} = -\frac{\sigma c_1}{a} \quad \text{and } \lambda_{24}(c) = -\frac{a(c_1 - c)}{c_1}. \tag{8}$$

It is clear that the eigenvalues $\lambda_{22}, \lambda_{23}$ are always negative since all the parameters of our model are positive. Moreover, $\lambda_{24}(c)$ is also negative, since its denominator is positive and its numerator is positive when E_2 exists from Proposition 3. Finally, $\lambda_{21}(c)$ is negative when $c > c_2$ and positive when $c < c_2$. □

Proposition 7 *Admissible equilibrium point E_3, when it does not coincide with E_2, is always unstable.*

Proof At the equilibrium point E_3, the Jacobian matrix becomes

$$\mathbf{J}(E_3; c) = \begin{bmatrix} -\frac{ab\theta_B}{m_T} & -\frac{c\theta_B}{m_T} & 0 & 0 \\ 0 & \frac{c\sigma m_T}{a\Theta_1} & \frac{a\gamma\Theta_1}{cm_T} & 0 \\ 0 & 0 & \frac{a\gamma\kappa\Theta_1}{\Theta_2} & -\frac{m_B\Theta_2}{a\gamma\Theta_1} \\ \frac{m_T(a\gamma\kappa\Theta_1 + \theta_R\Theta_2)}{m_B\Theta_2} & 0 & 0 & 0 \end{bmatrix},$$

with its characteristic polynomial being

$$\lambda^4 + \alpha_3\lambda^3 + \alpha_2\lambda^2 + \alpha_1\lambda + \alpha_0 = 0, \tag{9}$$

where

$$\begin{aligned} \alpha_0 &= -\frac{\theta_B(a\gamma\kappa\Theta_1 + \theta_R\Theta_2)}{m_T}, \\ \alpha_1 &= \frac{abc\gamma\kappa\sigma\theta_B}{\Theta_2}, \\ \alpha_2 &= -\frac{a^2b\gamma\kappa\theta_B\Theta_1}{m_T\Theta_2} + \frac{c\gamma\kappa\sigma m_T}{\Theta_2} - \frac{bc\sigma\theta_B}{\Theta_1}, \\ \alpha_3 &= -\frac{a\gamma\kappa\Theta_1}{\Theta_2} - \frac{c\sigma m_T}{a\Theta_1} + \frac{ab\theta_B}{m_T}. \end{aligned}$$

We utilise Descartes' rule of signs to prove our claim. Firstly, let $\alpha_0 \geq 0$, which means that

$$\frac{\theta_B}{m_T} \leq \frac{a\gamma\kappa + a\theta_N\theta_R - c\sigma\theta_R}{ab\gamma\kappa + ab\theta_N\theta_R} = \frac{c_1 - c}{bc_1},$$

which is impossible when E_3 exists and does not coincide with E_2 from Proposition 4. Hence, $\alpha_0 < 0$. Consequently, from Proposition 4, we have that when E_3 exists and does not coincide with E_2, then $\Theta_1 < 0$ and $\Theta_2 > 0$, which means that $\alpha_1, \alpha_2, \alpha_3 > 0$. Next, we apply the transformation

$$\lambda \mapsto -\lambda,$$

to (9), to get

$$\underbrace{\lambda^4}_{+}\underbrace{-\alpha_3\lambda^3}_{-}+\underbrace{\alpha_2\lambda^2}_{+}\underbrace{-\alpha_1\lambda}_{-}\underbrace{+\alpha_0}_{-}=0\,. \tag{10}$$

The sign changes in the sequence of the polynomial coefficients of (10) are three. Therefore, (10) has exactly one or three positive real roots, which means that (9) has exactly one or three negative real roots. In either case, (9) has at least one positive real root, so it follows that E_3 is unstable. □

We have yet to tackle the cases in which $E_1 \equiv E_2$ and $E_2 \equiv E_3$. When $c = c_1$, then $\lambda_{11}(c_1) = 0$, and when $c = c_2$, then $\lambda_{21}(c_2) = 0$, so in each case a one dimensional center manifold arises, and the linearisation theorem cannot be used. In order to determine the dynamics of our system in those two cases, we utilise the center manifold theorem (Jordan et al. 2007).

Proposition 8 *When $c = c_1$, then the equilibrium point $E_1 \equiv E_2$ is locally asymptotically stable.*

Proof For convenience, we firstly move the equilibrium point to the origin, using the transformation

$$\begin{aligned} T &\mapsto T + \overline{T} = T\,,\\ N &\mapsto N + \overline{N} = N + \frac{a}{c_1}\,,\\ R &\mapsto R + \overline{R} = R + \frac{\kappa}{\theta_R}\,,\\ B &\mapsto B + \overline{B} = B\,. \end{aligned} \tag{11}$$

After replacing (11) to system (1), while utilising that $c = c_1$, we get the transformed system

$$\frac{\mathrm{d}\mathbf{X}}{\mathrm{d}t} = \mathbf{A}_1\mathbf{X} + \mathbf{P_1}\,, \tag{12}$$

where

$$\mathbf{X} = \left[T, N, R, B\right]^{\mathsf{T}}\,,$$

$$\mathbf{A}_1 := \mathbf{J}(E_1; c = c_1) = \begin{bmatrix} 0 & 0 & 0 & 0\\ 0 & -\frac{\sigma c_1}{a} & -\frac{a\gamma}{c_1} & 0\\ 0 & 0 & -\theta_R & \frac{\kappa m_B}{\theta_R}\\ 0 & 0 & 0 & -\theta_B \end{bmatrix}$$

and

$$\mathbf{P}_1 = \left[-abT^2 - c_1TN, -\gamma RN, m_BBR, m_TTB\right]^{\mathsf{T}}\,.$$

$\mathbf{A}_1$ is upper diagonal, and its eigenvalues are $\lambda_{11}(c_1)$, λ_{12}, λ_{13} and λ_{14}, with corresponding eigenvectors $\mathbf{u}_{11}$, $\mathbf{u}_{12}$, $\mathbf{u}_{13}$ and $\mathbf{u}_{14}$, as given by (5)-(7).

We bring system (12) to its normal form with the help of the transformation

$$\mathbf{X} = \mathbf{U}_1\mathbf{Y}\,, \tag{13}$$

where we let

$$\mathbf{Y} = \left[y_1, y_2, y_3, y_4\right]^{\mathsf{T}} \quad \text{and} \quad \mathbf{U}_1 = \left[\mathbf{u}_{11}, \mathbf{u}_{12}, \mathbf{u}_{13}, \mathbf{u}_{14}\right].$$

By replacing (13) to system (12), we have that

$$\begin{aligned} &\mathbf{U}_1 \tfrac{\mathrm{d}\mathbf{Y}}{\mathrm{d}t} = \mathbf{A}_1 \mathbf{U}_1 \mathbf{Y} + \mathbf{P}_1 \\ \Leftrightarrow\ &\tfrac{\mathrm{d}\mathbf{Y}}{\mathrm{d}t} = \mathbf{U}_1^{-1} \mathbf{A}_1 \mathbf{U}_1 \mathbf{Y} + \mathbf{U}_1^{-1} P_1 \\ \Leftrightarrow\ &\tfrac{\mathrm{d}\mathbf{Y}}{\mathrm{d}t} = \mathbf{\Lambda}_1 \mathbf{Y} + \mathbf{F}_1 , \end{aligned} \tag{14}$$

where

$$\begin{aligned} &\mathbf{\Lambda}_1 = \mathrm{diag}(\lambda_{11}(c_1), \lambda_{12}, \lambda_{13}, \lambda_{14}) \quad \text{and} \\ &\mathbf{F}_1 = \left[f_{11}, f_{12}, f_{13}, f_{14}\right]^{\mathsf{T}} = \mathbf{U}_1^{-1} P \end{aligned}$$

$\mathbf{F}_1$ is a function of T, N, R and B. In order to express $\mathbf{F}_1$ as a function of y_1, y_2, y_3 and y_4, we substitute T, N, R and B from equation (13) to $\mathbf{F}_1$, to find that

$$\mathbf{F}_1 = \begin{bmatrix} -aby_1^2 + w_{11} y_1 y_2 + w_{12} y_1 y_3 - c_1 y_1 y_4 \\ m_T y_1 y_2 \\ w_{13} y_1 y_2 + w_{14} y_2^2 + m_B y_2 y_3 \\ w_{15} y_1 y_2 + w_{16} y_2 y_3 + w_{17} y_2^2 + w_{18} y_2 y_4 + w_{19} y_3^2 + w_{110} y_3 y_4 \end{bmatrix},$$

where w_{1i}, $i = 1, 2, 3, \ldots, 10$ are known constants.

Hence, system (14) can be written in the form

$$\frac{\mathrm{d}\mathbf{Y}}{\mathrm{d}t} = \begin{bmatrix} \mathbf{B}_1 & \mathbf{0} \\ \mathbf{0} & \mathbf{C}_1 \end{bmatrix} \mathbf{Y} + \mathbf{F}_1 ,$$

or equivalently

$$\frac{\mathrm{d}y_1}{\mathrm{d}t} = \mathbf{B}_1 y_1 + f_{11} , \tag{15a}$$

$$\begin{bmatrix} \frac{\mathrm{d}y_2}{\mathrm{d}t} \\ \frac{\mathrm{d}y_3}{\mathrm{d}t} \\ \frac{\mathrm{d}y_4}{\mathrm{d}t} \end{bmatrix} = \mathbf{C}_1 \begin{bmatrix} y_2 \\ y_3 \\ y_4 \end{bmatrix} + \begin{bmatrix} f_{12} \\ f_{13} \\ f_{14} \end{bmatrix}, \tag{15b}$$

where

$$\mathbf{B}_1 = \lambda_{11}(c_1) = 0 \quad \text{and} \quad \mathbf{C}_1 = \mathrm{diag}(\lambda_{12}, \lambda_{13}, \lambda_{14}) .$$

We have that $\mathbf{B}_1$ and $\mathbf{C}_1$ are constant matrices, with the eigenvalues of $\mathbf{B}_1$ having zero real part and the eigenvalues of $\mathbf{C}_1$ having negative real part, whereas f_{1i} is

smooth with $f_{1i}(0,0,0,0) = 0$ and $Df_{1i}(0,0,0,0) = 0$ for $i = 1,2,3,4$. From the center manifold theorem, there exists a center manifold which is parametrised by

$$\begin{bmatrix} y_2 \\ y_3 \\ y_4 \end{bmatrix} = \mathbf{h}_1(y_1) = \begin{bmatrix} h_{12}(y_1) \\ h_{13}(y_1) \\ h_{14}(y_1) \end{bmatrix},$$

with $\mathbf{h}_1(0) = 0$ and $D\mathbf{h}_1(0) = 0$, and satisfying

$$\mathbf{C}_1 \cdot \mathbf{h}_1(y_1) + \begin{bmatrix} f_{12}(y_1, \mathbf{h}_1(y_1)) \\ f_{13}(y_1, \mathbf{h}_1(y_1)) \\ f_{14}(y_1, \mathbf{h}_1(y_1)) \end{bmatrix} = D\mathbf{h}_1(y_1) \cdot [\mathbf{B}_1 y_1 + f_{11}(y_1, \mathbf{h}_1(y_1))],$$

while the flow on the center manifold is defined by the differential equation (15a).

Since $\mathbf{h}_1(0) = 0$ and $D\mathbf{h}_1(0) = 0$, then by approximating the center manifold with a Taylor series around 0, we get

$$\mathbf{h}_1(y_1) = \begin{bmatrix} b_{12}y_1^2 + b_{13}y_1^3 + b_{14}y_1^4 + O(y_1^5) \\ c_{12}y_1^2 + c_{13}y_1^3 + c_{14}y_1^4 + O(y_1^5) \\ d_{12}y_1^2 + d_{13}y_1^3 + d_{14}y_1^4 + O(y_1^5) \end{bmatrix}. \tag{16}$$

By replacing (16) to (15a) in order to express the terms of y_2, y_3, y_4 in f_{11}, we get

$$\frac{\mathrm{d}y_1}{\mathrm{d}t} = -aby_1^2 + O(y_1^3). \tag{17}$$

From $\mathbf{Y} = \mathbf{U}_1^{-1}\mathbf{X}$, we see that $y_1 = T$, so y_1 is non-negative. That means that 0 is an asymptotically stable point of equation (17), when approached from $y_1 \geq 0$ since $-ab < 0$. Thus, from the center manifold theorem, $\mathbf{0}$ is a locally asymptotically stable equilibrium of system (12), which proves the proposition. □

Proposition 9 *When $c = c_2$, then the equilibrium point $E_2 \equiv E_3$ is unstable.*

Proof For convenience, we firstly move the equilibrium point to the origin, using the transformation

$$\begin{aligned} T &\mapsto T + \overline{T} = T + \frac{c_1 - c}{bc_1}, \\ N &\mapsto N + \overline{N} = N + \frac{a}{c_1}, \\ R &\mapsto R + \overline{R} = R + \frac{\kappa}{\theta_R}, \\ B &\mapsto B + \overline{B} = B. \end{aligned} \tag{18}$$

After replacing (18) to system (1), while utilising that $c_2 = c$, we get the transformed system

$$\frac{\mathrm{d}\mathbf{X}}{\mathrm{d}t} = \mathbf{A}_2\mathbf{X} + \mathbf{P}_2, \tag{19}$$

where

$$\mathbf{X} = \left[T, N, R, B\right]^{\mathsf{T}},$$

$$\mathbf{A}_2 := \mathbf{J}(E_2; c = c_2) = \begin{bmatrix} -\frac{a(c_1-c_2)}{c_1} & -\frac{c_2(c_1-c_2)}{bc_1} & 0 & 0 \\ 0 & -\frac{\sigma c_1}{a} & -\frac{a\gamma}{c_1} & 0 \\ 0 & 0 & -\theta_R & \frac{\kappa m_B}{\theta_R} \\ 0 & 0 & 0 & 0 \end{bmatrix}$$

and

$$\mathbf{P}_2 = \left[-abT^2 - c_2TN, -\gamma RN, m_B BR, m_T TB\right]^{\mathsf{T}}.$$

$\mathbf{A}_2$ is upper diagonal, so its eigenvalues are $\lambda_{21}(c_2)$, λ_{22}, λ_{23} and $\lambda_{24}(c_2)$ with corresponding eigenvectors

$$\begin{aligned} \mathbf{u}_{21} &= \left[\tfrac{a\gamma\kappa c_2 m_B}{b\theta_R^2\sigma c_1^2}, -\tfrac{a^2\gamma\kappa m_B}{\theta_R^2\sigma c_1^2}, \tfrac{\kappa m_B}{\theta_R^2}, 1\right]^{\mathsf{T}}, \\ \mathbf{u}_{22} &= \left[\tfrac{a^2c_2\gamma(c_1-c_2)}{bc_1(a(c_1-c_2)-\theta_R c_1)(\sigma c_1 - a\theta_R)}, \tfrac{a^2\gamma}{c_1(a\theta_R-\sigma c_1)}, 1, 0\right]^{\mathsf{T}}, \\ \mathbf{u}_{23} &= \left[-\tfrac{ac_2(c_1-c_2)}{b(a^2(c_1-c_2)-\sigma c_1^2)}, 1, 0, 0\right]^{\mathsf{T}} \quad \text{and } \mathbf{u}_{24} = \left[1, 0, 0, 0\right]^{\mathsf{T}}. \end{aligned} \tag{20}$$

We transform system (19) to its normal form with the help of the transformation

$$\mathbf{X} = \mathbf{U}_2\mathbf{Y}, \tag{21}$$

where we let

$$\mathbf{U}_2 = \left[\mathbf{u}_{21}, \mathbf{u}_{22}, \mathbf{u}_{23}, \mathbf{u}_{24}\right].$$

By replacing (21) to system (19), we get

$$\frac{\mathrm{d}\mathbf{Y}}{\mathrm{d}t} = \mathbf{\Lambda}_2\mathbf{Y} + \mathbf{F}_2, \tag{22}$$

where

$$\mathbf{\Lambda_2} = \mathrm{diag}(\lambda_{21}(c_2), \lambda_{22}, \lambda_{23}, \lambda_{24}(c_2)) \quad \text{and} \quad \mathbf{F}_2 = \left[f_{21}, f_{22}, f_{23}, f_{24}\right]^{\mathsf{T}} = \mathbf{U}_2^{-1}\mathbf{P}_2.$$

By using equation (21) and substituting T, N, R and B to $\mathbf{F}_2$, we find that

$$\begin{aligned} f_{21} &= w_{21}y_1^2 + w_{22}y_1y_2 + w_{23}y_1y_3 - m_T y_1y_4, \\ f_{22} &= w_{24}y_1^2 + w_{25}y_1y_2 + w_{26}y_1y_3 - w_{27}y_1y_4, \\ f_{23} &= w_{28}y_1^2 + w_{29}y_2^2 + \gamma y_2y_3 + w_{210}y_1y_2 + w_{211}y_1y_3 - w_{212}y_1y_4, \\ f_{24} &= w_{213}y_1^2 + w_{214}y_2^2 + w_{215}y_3^2 + w_{216}y_3y_4 + aby_4^2 + w_{217}y_2y_3 \\ &\quad + w_{216}y_2y_4 + w_{217}y_1y_2 + w_{218}y_1y_3 - w_{219}y_1y_4, \end{aligned}$$

where w_{2i}, $i = 1, 2, 3, \ldots, 19$ are known constants.

Hence, system (22) can be written in the form

$$\frac{\mathrm{d}\mathbf{Y}}{\mathrm{d}t} = \begin{bmatrix} \mathbf{B}_2 & \mathbf{0} \\ \mathbf{0} & \mathbf{C}_2 \end{bmatrix} \mathbf{Y} + \mathbf{F}_2 \,,$$

or equivalently

$$\frac{\mathrm{d}y_1}{\mathrm{d}t} = \mathbf{B}_2 y_1 + f_{21} \,, \tag{23a}$$

$$\begin{bmatrix} \frac{\mathrm{d}y_2}{\mathrm{d}t} \\ \frac{\mathrm{d}y_3}{\mathrm{d}t} \\ \frac{\mathrm{d}y_4}{\mathrm{d}t} \end{bmatrix} = \mathbf{C}_2 \begin{bmatrix} y_2 \\ y_3 \\ y_4 \end{bmatrix} + \begin{bmatrix} f_{22} \\ f_{23} \\ f_{24} \end{bmatrix} , \tag{23b}$$

where

$$\mathbf{B}_2 = \lambda_{21}\,(c_2) = 0 \quad \text{and} \quad \mathbf{C}_2 = \mathrm{diag}(\lambda_{22}, \lambda_{23}, \lambda_{24}\,(c_2)) \,.$$

We have that $\mathbf{B}_2$ and $\mathbf{C}_2$ are constant matrices, with the eigenvalues of $\mathbf{B}_2$ having 0 real part and the eigenvalues of $\mathbf{C}_2$ having negative real part, whereas f_{2i} is smooth with $f_{2i}(0,0,0,0) = 0$ and $Df_{2i}(0,0,0,0) = 0$ for $i = 1, 2, 3, 4$. By the center manifold theorem, there exists a center manifold which is parametrised by

$$\begin{bmatrix} y_2 \\ y_3 \\ y_4 \end{bmatrix} = \mathbf{h}_2(y_1) = \begin{bmatrix} h_{22}(y_1) \\ h_{23}(y_1) \\ h_{24}(y_1) \end{bmatrix} ,$$

with $\mathbf{h}_2(0) = 0$ and $D\mathbf{h}_2(0) = 0$, and satisfying

$$\mathbf{C}_2 \cdot \mathbf{h}_2(y_1) + \begin{bmatrix} f_{22}(y_1, \mathbf{h}_2(y_1)) \\ f_{23}(y_1, \mathbf{h}_2(y_1)) \\ f_{24}(y_1, \mathbf{h}_2(y_1)) \end{bmatrix} = D\mathbf{h}_2(y_1) \cdot [\mathbf{B}_2 y_1 + f_{21}(y_1, \mathbf{h}_2(y_1))] \,,$$

while the flow on the center manifold is defined by the differential equation (23a).

Since $\mathbf{h}_2(0) = 0$ and $D\mathbf{h}_2(0) = 0$, then by approximating the center manifold with a Taylor series around 0, we get

$$\mathbf{h}_2(y_1) = \begin{bmatrix} b_{22} y_1^2 + b_{23} y_1^3 + b_{24} y_1^4 + O(y_1^5) \\ c_{22} y_1^2 + c_{23} y_1^3 + c_{24} y_1^4 + O(y_1^5) \\ d_{22} y_1^2 + d_{23} y_1^3 + d_{24} y_1^4 + O(y_1^5) \end{bmatrix} . \tag{24}$$

By replacing (24) to (23a) in order to express the terms of y_2, y_3, y_4 in f_{21}, we get

$$\frac{\mathrm{d}y_1}{\mathrm{d}t} = w_{21} y_1^2 + O(y_1^3) \,, \tag{25}$$

with

$$w_{21} = \frac{c_2 \gamma \kappa \sigma m_B m_T}{ab\,(\gamma k + \theta_N \theta_R)^2} > 0 \,.$$

From $\mathbf{Y} = \mathbf{U}_2^{-1}\mathbf{X}$, we see that $y_1 = B$, so y_1 is non-negative. That means that 0 is an unstable equilibrium point of equation (25), when approached from $y_1 \geq 0$ since $w_{21} > 0$. Thus, from the center manifold theorem, $\mathbf{0}$ is an unstable equilibrium point of system (19), which proves the proposition. □

Having studied every possible case in which the equilibrium points are biologically realistic, we conclude with the main result of the present section as follows.

Proposition 10 *(Local stability analysis) For the admissible equilibrium points of system (1), the following facts hold true.*

- *E_1 always exists, and is locally stable when $c \geq c_1$, and unstable when $c < c_1$.*
- *E_2 exists when $c < c_1$, and is locally stable when $c \geq c_2$, and unstable when $c < c_2$.*
- *E_3 exists when $c > c_2$ and $\frac{\theta_B}{m_T} < \frac{1}{b}$, and is always unstable.*
- *$E_1 \equiv E_2$ when $c = c_1$, and $E_2 \equiv E_3$ when $c = c_2$.*

4 Bifurcation Analysis

Starting off, we prove that, under certain sufficient conditions, IVP has no closed orbits and therefore a Hopf bifurcation cannot occur.

Proposition 11 (Lack of Hopf bifurcations) *If*

$$0 \leq T_0 \leq \frac{1}{b} \text{ and } \frac{\theta_B}{m_T} > \frac{1}{b},$$

then IVP has no closed orbits.

Proof From (1d) along with the non-negativity of the solution (see Proposition 14) we get that

$$\operatorname{sgn}\frac{\mathrm{d}B}{\mathrm{d}t} = \operatorname{sgn}\left(T - \frac{\theta_B}{m_T}\right).$$

Since $T_0 \leq 1/b$, we have from Proposition 15 that $T \leq 1/b$, as well. Hence, by

$$\frac{\theta_B}{m_T} > \frac{1}{b}$$

we get that B is strictly decreasing, therefore there are no periodic solutions of non-zero period, i.e no closed orbits. □

Remark 2 A different way to prove the lack of Hopf bifurcation is by supposing that there is a periodic solution (T, N, R, B) of period $P \neq 0$, hence every component

is also P-periodic function. Then, from (A1) we get that $e^{\int_0^t (m_T T(s) - \theta_B)\,\mathrm{d}s}$ is also P-periodic, and so does

$$\int_0^t \left(T(s) - \frac{\theta_B}{m_T} \right) \mathrm{d}s.$$

From this, along with the fact that $m_T T - \theta_B$ is P-periodic, we get that

$$\int_0^P \left(T(s) - \frac{\theta_B}{m_T} \right) \mathrm{d}s = 0.$$

Dealing as before, we have a contradiction, since

$$T - \frac{\theta_B}{m_T} \leq \frac{1}{b} - \frac{\theta_B}{m_T} < 0.$$

The result of Proposition 10 makes us suspect that two transcritical bifurcations are happening; one between E_1 and E_2 when $c = c_1$, and one between E_2 and E_3 when $c = c_2$. Indeed, we set the right-hand side of system (1) equal to $\mathbf{G}$, i.e.

$$\mathbf{G}(T, N, R, B) := \begin{bmatrix} aT(1 - bT) - cNT \\ \sigma - \theta_N N - \gamma RN \\ \kappa - \theta_R R + m_B BR \\ -\theta_B B + m_T TB \end{bmatrix},$$

and we use Sotomayor's theorem (Perko 2006) to prove our observations.

Proposition 12 (Transcritical bifurcation 1) *System (1) experiences a transcritical bifurcation at the equilibrium point $E_1 \equiv E_2$ as the parameter c varies through c_1.*

Proof The Jacobian matrix of system (1) at $E_1 \equiv E_2$, i.e. when $c = c_1$, is given by $\mathbf{A}_1$. From (5) and (6), we see that the eigenvector corresponding to the zero eigenvalue is $\mathbf{u}_{11}$, whereas simple computations show us that the eigenvector corresponding to the zero eigenvalue of matrix $\mathbf{A}_1^{\mathsf{T}}$ is $\mathbf{w}_1 = \left[1, 0, 0, 0\right]^{\mathsf{T}}$.

Furthermore, we have that

$$\frac{\partial \mathbf{G}(T, N, R, B; c)}{\partial c} = \left[-NT, 0, 0, 0\right]^{\mathsf{T}},$$
$$D\frac{\partial \mathbf{G}(T, N, R, B; c)}{\partial c}\mathbf{u}_{11} = \left[-N, 0, 0, 0\right]^{\mathsf{T}},$$

and

$$D^2\mathbf{G}(T, N, R, B)(\mathbf{u}_{11}, \mathbf{u}_{11}) = \left[-2ab, 0, 0, 0\right]^{\mathsf{T}}.$$

Consequently, when $c = c_1$ we have that

$$\mathbf{w}_1^{\mathsf{T}} \frac{\partial \mathbf{G}(E_1; c_1)}{\partial c} = 0,$$

$$\mathbf{w}_1^{\mathsf{T}}\left[D\frac{\partial \mathbf{G}(E_1;c_1)}{\partial c}\mathbf{u}_{11}\right] = -\frac{a}{c_1} \neq 0\,,$$
$$\mathbf{w}_1^{\mathsf{T}}\left[D^2\mathbf{G}(E_1;c_1)(\mathbf{u}_{11},\mathbf{u}_{11})\right] = -2ab \neq 0\,.$$

Thus, the conditions of Sotomayor's theorem are satisfied and the proposition is proved. □

Proposition 13 (Transcritical bifurcation 2) *System (1) experiences a transcritical bifurcation at the equilibrium point $E_2 \equiv E_3$ as the parameter c varies through c_2.*

Proof Since

$$c = c_2 \Leftrightarrow \theta_B = \frac{a\theta_N m_T \theta_R + a\gamma\kappa m_T - c\sigma m_T \theta_R}{ab\gamma\kappa + ab\theta_N\theta_R} =: \theta_B^*\,,$$

we prove the equivalent proposition of system (1) experiencing a transcritical bifurcation at the equilibrium point $E_2 \equiv E_3$ as the parameter θ_B varies through θ_B^*, as the conditions of Sotomayor's theorem cannot be satisfied in the case of parameter c varying through c_2.

We have that the Jacobian of system (1) at $E_2 \equiv E_3$, i.e. when $\theta_B = \theta_B^*$, is equal to $\mathbf{A}_2 = \mathbf{J}(E_2; c = c_2) = \mathbf{J}(E_2; \theta_B = \theta_B^*)$.

From (8) and (20), we see that the eigenvector corresponding to the zero eigenvalue is $\mathbf{u}_{21}$, whereas simple computations show us that the eigenvector corresponding to the zero eigenvalue of matrix $\mathbf{A}_2^{\mathsf{T}}$ is $\mathbf{w}_2 = \left[0, 0, 0, 1\right]^{\mathsf{T}}$.

Furthermore, we have that

$$\frac{\partial \mathbf{G}(T, N, R, B; \theta_B)}{\partial \theta_B} = \left[0, 0, 0, -B\right]^{\mathsf{T}},$$
$$D\frac{\partial \mathbf{G}(T, N, R, B; \theta_B)}{\partial \theta_B}\mathbf{u}_{21} = \left[0, 0, 0, -1\right]^{\mathsf{T}},$$

and

$$D^2\mathbf{G}(T, N, R, B; \theta_B)(\mathbf{u}_{21}, \mathbf{u}_{21}) = \left[0, \frac{2\gamma^2\kappa^2\sigma m_B^2}{\theta_R^2(\gamma\kappa+\theta_N\theta_R)^2}, \frac{2\kappa m_B^2}{\theta_R^2}, \frac{2c\gamma\kappa\sigma m_B m_T}{ab(\gamma\kappa+\theta_N\theta_R)^2}\right]^{\mathsf{T}}.$$

Consequently, when $\theta_B = \theta_B^*$ we have that

$$\mathbf{w}_2^{\mathsf{T}}\frac{\partial \mathbf{G}(E_2;\theta_B^*)}{\partial \theta_B} = 0\,,$$
$$\mathbf{w}_2^{\mathsf{T}}\left[D\frac{\partial \mathbf{G}(E_2;\theta_B^*)}{\partial \theta_B}\right] = -1 \neq 0\,,$$
$$\mathbf{w}_2^{\mathsf{T}}\left[D^2\mathbf{G}(E_2;\theta_B^*)(\mathbf{u}_{21},\mathbf{u}_{21})\right] = \frac{2c\gamma\kappa\sigma m_B m_T}{ab\,(\gamma\kappa+\theta_N\theta_R)^2} \neq 0\,.$$

Thus, the conditions of Sotomayor's theorem are satisfied and the proposition is proved. □

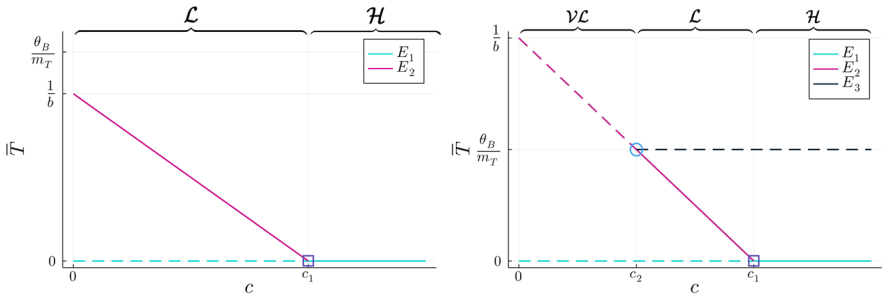

(a) The tumour carrying capacity is bounded from above, i.e. $\frac{\theta_B}{m_T} \geq \frac{1}{b}$.

(b) The tumour carrying capacity is bounded from below, i.e. $\frac{\theta_B}{m_T} < \frac{1}{b}$.

Fig. 3 Projection of the bifurcation diagram of system (1) onto the $\overline{T}$–c plane. Solid line (—): Stable equilibrium. Dashed line (- -): Unstable equilibrium. □: Transcritical bifurcation 1. ◯: Transcritical bifurcation 2. $\mathcal{VL}$: Region in which c is "very low", i.e. $c < c_2$ when $c_2 > 0$. $\mathcal{L}$: Region in which c is "low", i.e. $c < c_1$ when $c_2 < 0$ and $c_2 < c < c_1$ when $c_2 > 0$. $\mathcal{H}$: Region in which c is "high", i.e. $c > c_1$ (Color figure online)

The value and stability of the first coordinate—that is the breast cancer cell population—at equilibrium, depending on parameter c is given in Fig. 3.

5 Numerical Simulations

In this section, we numerically solve our model, using Julia and the suite DifferentialEquations.jl (Rackauckas and Nie 2017), under two antipodal theoretical scenarios concerning the absence and the presence of tBregs. Contrary to our previous local stability analysis, numerical simulations help us develop an intuition about the global behaviour of our model. Additionally, we perform numerical parameter sensitivity analysis, in order to further explore the dependence of the solution of our model to its parameters, under different initial conditions of tBregs.

The parameter values used in our simulations are listed in Table 2, unless otherwise stated, and their derivation is explained in is explained in Appendix B. In particular, m_T either becomes

$$m_T = m_T^A := 5 \cdot 10^{-15} \text{ cell}^{-1} \cdot \text{day}^{-1} ,$$

or

$$m_T = m_T^B := 5 \cdot 10^{-10} \text{ cell}^{-1} \cdot \text{day}^{-1} .$$

Thus, choosing the value m_T^A yields $\frac{\theta_B}{m_T} > \frac{1}{b}$, whereas choosing the value m_T^B yields $\frac{\theta_B}{m_T} < \frac{1}{b}$, allowing us to explore the different dynamics of IVP.

Considering the values of the two bifurcation points of system (1) with respect to parameter c, we have that $c_1 = 2.88 \cdot 10^{-10}$ cell^{-1} · day^{-1}, since c_1 is independent from the value of m_T. When $m_T = m_T^A$, then $c_2 < 0$, as expected from our bifurcation analysis, whereas when $m_T = m_T^B$, then $c_2 = 5.76 \cdot 10^{-11}$ cell^{-1} · day^{-1}.

Finally, we choose $N_0 = 5 \cdot 10^8$ cells and $R_0 = 2 \cdot 10^8$ cells.

Table 2 Units and values of the parameters of system (1). For estimations arising from literature see Appendix B

Prm.	Unit	Value	Source
a	day^{-1}	0.15	Bitsouni and Tsilidis (2022)
b	cell^{-1}	$1 \cdot 10^{-9}$	Bitsouni and Tsilidis (2022)
c	$\text{cell}^{-1} \cdot \text{day}^{-1}$	Varied	–
σ	$\text{cell} \cdot \text{day}^{-1}$	$5 \cdot 10^{7}$	Estimated from Zhang et al. (2007)
θ_N	day^{-1}	0.07	Estimated from Zhang et al. (2007)
γ	$\text{cell}^{-1} \cdot \text{day}^{-1}$	$1 \cdot 10^{-10}$	Estimated from equilibrium point
κ	$\text{cell} \cdot \text{day}^{-1}$	$1 \cdot 10^{7}$	Estimated from equilibrium point
θ_R	day^{-1}	0.03851	Estimated from Mabarrack et al. (2008)
m_B	$\text{cell}^{-1} \cdot \text{day}^{-1}$	$3 \cdot 10^{-8}$	No data found
θ_B	day^{-1}	0.4	No data found
m_T	$\text{cell}^{-1} \cdot \text{day}^{-1}$	Varied	–

5.1 The Scenario of Absent tBregs ($B_0 = 0$)

As can be seen from equation (A1), when $B_0 = 0$, we have that $B(t) = 0,\ t \in \mathbb{R}_{\geq 0}$. Therefore, system (1) becomes a 3D system with only breast cancer cells, NK cells and Tregs existing in the body.

Plotting the phase portrait of the resulting 3D system, for different values of c, we get Fig. 4. We notice that all trajectories move towards an equilibrium point for all c. This equilibrium point moves along the line

$$\{(T, N, R) \in \mathbb{R}^3_{\geq 0} : N = \frac{\sigma\theta_R}{\gamma\kappa + \theta_N\theta_R}, R = \frac{\kappa}{\theta_R}\},$$

with T getting bigger, as c gets smaller, and vice versa. When $c > c_1$, T reaches zero. We observe the same type of transcritical bifurcation that happens between E_1 and E_2 when $c = c_1$ for system (1), also happens for the 3D system. Even with no rigorous result at hand regarding the global stability of IVP with tBregs no longer in the picture, it is apparent that for the 3D system the equilibrium point E_1 is globally stable when $c > c_1$ and E_2 is globally stable when $c < c_1$. The crux of the scenario in question is:

Conclusion 1_a:
In the absence of tBregs, the breast tumour will reach its carrying capacity due to NK cell insufficiency, i.e. $T \nearrow \frac{1}{b}$ when $c \searrow 0$.

5.2 The Scenario of Present tBregs ($B_0 \neq 0$)

In this section, we study the scenario in which the initial condition of tBregs is not 0. We divide our analysis into three sections: Sect. 5.2.1 in which $m_T = m_T^A$ and

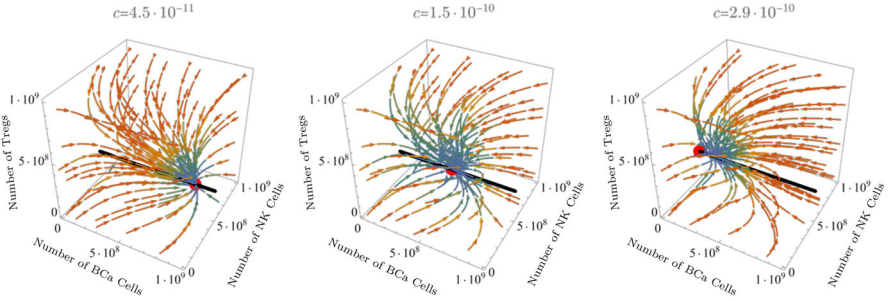

Fig. 4 Phase portrait of system (1) with $B_0 = 0$, for different values of c. The equilibrium point $(\overline{T}, \overline{N}, \overline{R})$ pictured by the red sphere moves along the black line, which is given by $\{(T, N, R) \in \mathbb{R}^3_{\geq 0} : N = \frac{\sigma\theta_R}{\gamma\kappa+\theta_N\theta_R}, R = \frac{\kappa}{\theta_R}\}$. The value of $\overline{T}$ tends to 0, as c increases, whereas tends to $\frac{1}{b}$, as c tends to 0 (Color figure online)

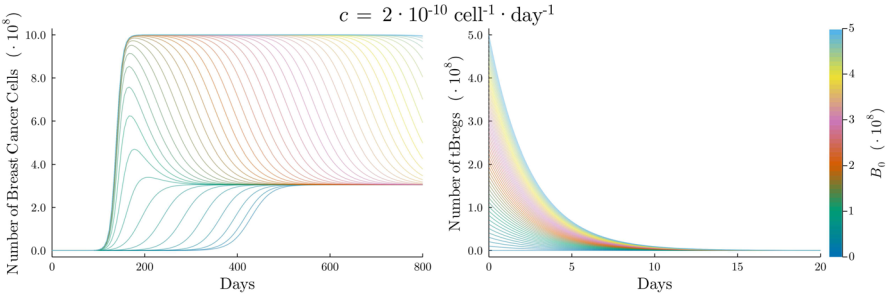

Fig. 5 Ensemble simulations of IVP, with B_0 taking values in the 30-point discretisation of the interval $\left[0, 5 \cdot 10^8\right] \cdot$ cells, $T_0 = 5$ cells, and $c = 2 \cdot 10^{-10}$ cell^{-1} $\cdot$ day^{-1} (region $\mathcal{L}$). When $B \to 0$, T eventually tends to $\overline{T} > 0$ of E_2 (Color figure online)

therefore $\frac{\theta_B}{m_T} \geq \frac{1}{b}$, and Sect. 5.2.2 in which $m_T = m_T^B$ and therefore $\frac{\theta_B}{m_T} < \frac{1}{b}$. In both first sections, we individually study each of the involved regions, $\mathcal{VL}$, $\mathcal{L}$ and $\mathcal{H}$, admitted by our bifurcation analysis and depicted in Fig. 3. In Sect. 5.2.3 we investigate the influence of the rate of NK-induced breast cancer cell death, c, to our model.

5.2.1 Bounded-From-Above Tumour Carrying Capacity ($\frac{\theta_B}{m_T} \geq \frac{1}{b}$)

Here, we show that the dynamics of the solution of IVP are eventually the same with the ones of the previous scenario. However, there are interesting differences between the two scenarios.

When $m_T = m_T^A$, we have that $\frac{\theta_B}{m_T} \geq \frac{1}{b}$, which means that B is strictly decreasing. Additionally, only equilibria E_1 and E_2 exist. Figs. 5 and 6 depict both T and B, for c in region $\mathcal{L}$ and $\mathcal{H}$, respectively. As can be seen in the aforementioned figures, T forms a single peak, which increases as B_0 increases. Such an increase of T continues until T reaches its carrying capacity, $\frac{1}{b}$, and after that it gradually flattens out. The greater B_0 is, the longer T stays close to $\frac{1}{b}$, before eventually tending to $\overline{T}$ of E_2. Consequently, as B_0 increases, the metastatic potential becomes higher. This comes

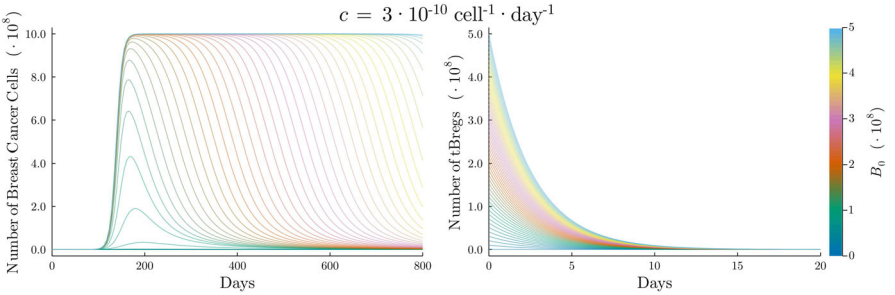

Fig. 6 Ensemble simulations of IVP, with B_0 taking values in the 30-point discretisation of the interval $\left[0, 5 \cdot 10^8\right] \cdot$ cells , $T_0 = 5$ cells, and $c = 3 \cdot 10^{-10}$ cell$^{-1} \cdot$ day^{-1} (region $\mathcal{H}$). When $B \to 0$, T eventually tends to $\overline{T} = 0$ of E_1 (Color figure online)

in agreement with the results of Olkhanud et al. (2011), where tBregs were associated with breast cancer metastasising to the lungs.

In Fig. 6, T eventually vanishes, instead of tending to a positive value, as in Fig. 5. Thus, in the light of Fig. 4, when $B \to 0$, the dynamics of IVP are similar to the corresponding ones of the problem with the simplified 3D system for $B = 0$.

All in all, we reach the following conclusion:

Conclusion 2:
In the presence of tBregs, if tumour carrying capacity is bounded from above, then the breast tumour will initially reach its carrying capacity due to the effect of tBregs, i.e. initially $T \nearrow \frac{1}{b}$ when $B_0 \nearrow$.

5.2.2 Bounded-From-Bellow Tumour Carrying Capacity ($\frac{\theta_B}{m_T} < \frac{1}{b}$)

When $\frac{\theta_B}{m_T} < \frac{1}{b}$, B can become an increasing function. Hence, even if tBregs start as just a few cells, they could cause breast cancer cells to reach their carrying capacity.

Region $\mathcal{L}$

When $c = 9 \cdot 10^{-11}$ cell$^{-1} \cdot$ day^{-1}, we have that $c_2 < c < c_1$. Depending on the initial condition of tBregs, the dynamics of IVP vary greatly. When $B_0 = 5 \cdot 10^5$ cells, we get Fig. 7. In Fig. 7, we see that tBregs, despite increasing up until around the 20th day, are unable to continue doing so and are eventually depleted. tBreg levels did not reach a sufficient population number that would allow breast cancer cells to grow to their carrying capacity. Instead, breast cancer cells stabilise to equilibrium point E_2.

Increasing the initial condition of tBregs to $B_0 = 5 \cdot 10^6$ cells, we get Fig. 8. In Fig. 8, we see that when the initial breast cancer cell population is around $6 \cdot 10^8$ cells, tBregs do not get depleted. Additionally, in every simulation where tBregs do not deplete, they cause breast cancer cells to move away from equilibrium point E_2 and reach their carrying capacity.

Region $\mathcal{VL}$

When $c = 2 \cdot 10^{-11}$ cell$^{-1} \cdot$ day^{-1}, we have that $c < c_2$. Region $\mathcal{VL}$ is a particular interesting case, since our local stability analysis showed that both E_1 and E_2 are

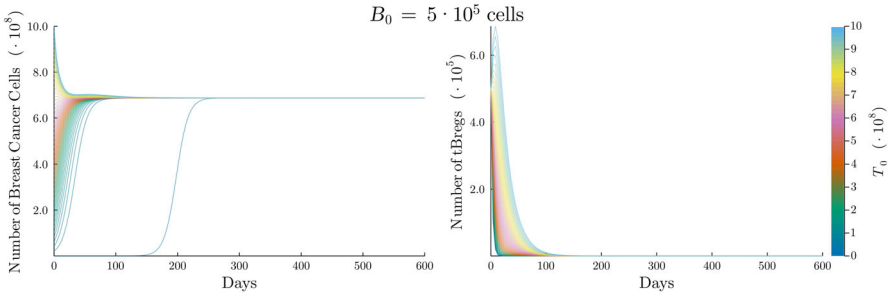

Fig. 7 Ensemble simulations of IVP, with T_0 taking values in the 50-point discretisation of the interval $\left[0, 10^9\right]$ · cells, $c = 9 \cdot 10^{-11}$ cell^{-1} · day^{-1} and $B_0 = 5 \cdot 10^5$ cells. Left: Number of tBregs. Right: Number of breast cancer cells. We notice that when $B_0 = 5 \cdot 10^5$ cells, the trajectories of our model move towards E_2 (Color figure online)

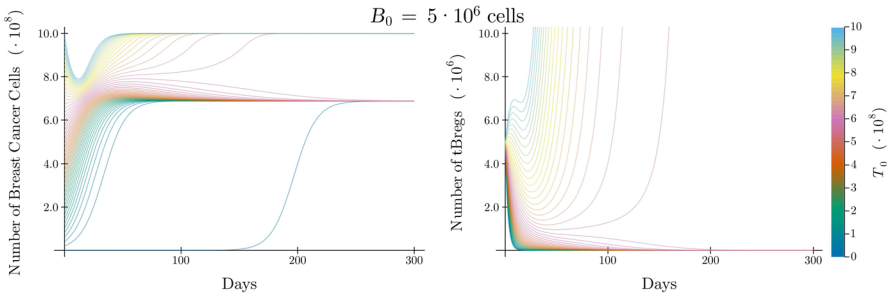

Fig. 8 Ensemble simulations of IVP, with T_0 taking values in the 50-point discretisation of the interval $\left[0, 10^9\right]$ · cells, $c = 9 \cdot 10^{-11}$ cell^{-1} · day^{-1} and $B_0 = 5 \cdot 10^6$ cells. Left: Number of breast cancer cells. Right: Number of tBregs. We notice that, unlike the corresponding simulations of Fig. 7, when $B_0 = 5 \cdot 10^6$ cells, and if $T_0 \geq 6 \cdot 10^8$, then the breast tumour reaches its carrying capacity (Color figure online)

unstable, hence making the dynamics of IVP difficult to determine without numerical simulations. In Fig. 9, we notice that despite the initial number of tBregs being as low as $B_0 = 50$ cells, tBregs manage to proliferate. Even though up until around the 200th day breast cancer cells seem to have stabilised at equilibrium point E_2, they proceed to start increasing up until they reach their carrying capacity. An interesting observation is that tBreg levels need to be around 10^8 cells in order for breast cancer cells to reach their carrying capacity, much like the case studied for the scenario of $\frac{\theta_B}{m_T} \geq \frac{1}{b}$ in Fig. 6.

Finally, we notice that when tBregs are scarce, even if the initial number of breast cancer cells is very close to the tumour carrying capacity, breast cancer cells are not able to maintain their high levels and decrease until they reach E_2. However, this changes when tBregs become around 10^8 cells, causing breast cancer cells to increase to their carrying capacity, while also being able to maintain their high numbers.

Region $\mathcal{H}$

When $c = 3 \cdot 10^{-10}$ cell^{-1} · day^{-1}, we have that $c > c_1$. In this case, the ability of NK cells at lysing breast cancer cells is at its highest, so we expect some of our

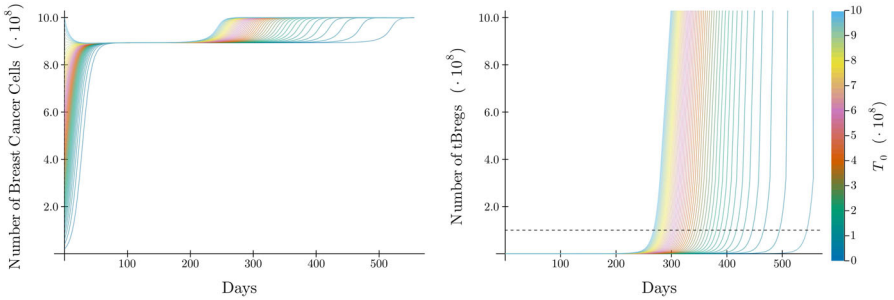

Fig. 9 Ensemble simulations of IVP, with T_0 taking values in the 50-point discretisation of the interval $\left[0, 10^9\right]$ · cells, $c = 2 \cdot 10^{-11}$ cell^{-1} · day^{-1} and $B_0 = 50$ cells. Left: Number of breast cancer cells. Right: Number of tBregs. Even though breast cancer cells seem to have stabilised to their corresponding E_2 value for more than 100 days in each simulation, when tBerg levels are about 10^8 cells (dashed line), breast cancer cells start increasing again and reach their carrying capacity (Color figure online)

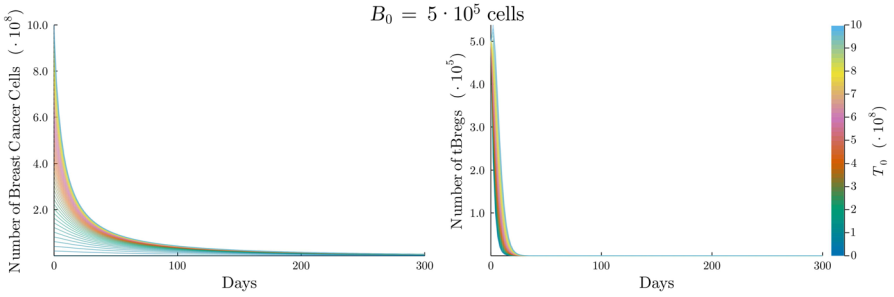

Fig. 10 Ensemble simulations of IVP, with T_0 taking values in the 50-point discretisation of the interval $\left[0, 10^9\right]$ · cells, $c = 3 \cdot 10^{-10}$ cell^{-1} · day^{-1} and $B_0 = 5 \cdot 10^5$ cells. Left: Number of breast cancer cells. Right: Number of tBregs. We notice that breast cancer cells are quickly depleted from the body when $c = 3 \cdot 10^{-10}$ cell^{-1} · day^{-1} ($c > c_1$) and $B_0 = 5 \cdot 10^5$ cells (Color figure online)

simulations to result in the elimination of the tumour. As anticipated, we see that in Fig. 10, when the initial condition of tBregs is $B_0 = 5 \cdot 10^5$, breast cancer cells, along with tBregs, are quickly depleted from the body for all simulations.

However, the same does not hold if the initial number of tBergs is higher. When the initial condition of IVP becomes equal to equilibrium point E_3, which in this case is equal to $\left(8 \cdot 10^8, 6 \cdot 10^7, 7.63 \cdot 10^9, 1.24 \cdot 10^6\right)$ · cells, we get Fig. 11. In Fig. 11, we observe that when the initial condition of breast cancer cells is lower than the value of breast cancer cells at E_3, the tumour is eliminated, whereas if it is higher, the tumour reaches its carrying capacity. Naturally, if it is equal to the value of breast cancer cells at E_3, then the solution is constant. Even though the trajectories that move towards the tumour carrying capacity do not actually move towards an equilibrium point, a sort of bistability phenomenon appears, as far as the population of breast cancer cells is concerned.

Throughout Sect. 5.2, we observed the importance of tBergs in the dynamics of IVP. Each time tBreg levels were sufficiently high, breast cancer cells reached their carrying capacity. In the presence of tBregs, breast tumour can reach its carrying

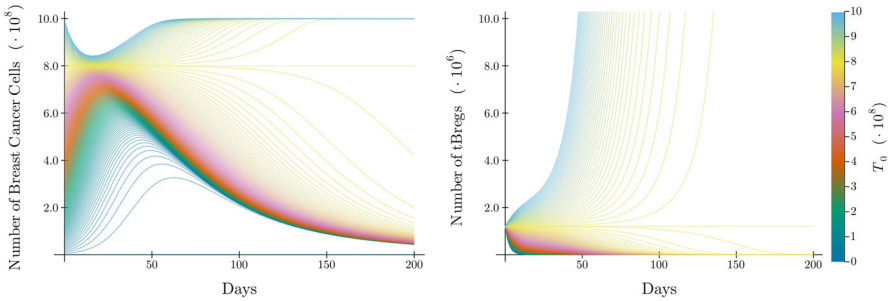

Fig. 11 Ensemble simulations of IVP, with T_0 taking values in the 200-point discretisation of the interval $\left[0, 10^9\right]$ · cells, $c = 3 \cdot 10^{-10}$ cell^{-1} · day^{-1} and $(T_0, N_0, R_0, B_0) = E_3$ cells. Left: Number of breast cancer cells. Right: Number of tBregs. We notice that if T_0 is higher than the corresponding value of T in E_3 then $T \nearrow \frac{1}{b}$, whereas if T_0 is lower than the corresponding value of T in E_3 then $T \searrow 0$ (Color figure online)

capacity independently of the value of parameter c. Hence, we reach the following conclusion:

Conclusion 3:
In the presence of tBregs, if tumour carrying capacity is bounded from below, then the breast tumour will eventually reach its carrying capacity due to the effect of an increasing population of tBregs, i.e. $T \nearrow \frac{1}{b}$ when $B \nearrow$.

5.2.3 The Importance of *c*

Our bifurcation analysis, along with our numerical simulations, underlined the importance of the rate at which NK cells lyse breast cancer cells. A way to numerically visualise the bifurcation diagram of Fig. 3 is with Fig. 12. In Fig. 12, we let c take a range of values between $4 \cdot 10^{-11}$ and $4 \cdot 10^{-10}$ · cell^{-1} · day^{-1}, while keeping the initial condition constant. As expected from our stability and numerical analysis, when $c < c_1$, breast cancer cells increase until they reach their carrying capacity. Additionally, when $c_1 < c < c_2$ equilibrium point E_2 is stable, and the value of breast cancer cells at the equilibrium decreases, as we increase the value of c, until it reaches 0, when $c > c_2$.

Additionally, when the value of c is a bit smaller than c_2, our model predicts breast cancer cells decreasing to a very small, but nonzero, amount. This clinically undetectable population could seize its proliferation, until the tumour micro-environmental conditions are suitable for its growth. This phenomenon is known as cancer dormancy and it happens to 20-45% of breast cancer patients (Aguirre-Ghiso 2007).

To sum up, similarly to Conclusion 1_a we have that:

Conclusion 1_p:
In the presence of tBregs, the breast tumour will reach its carrying capacity due to NK cell insufficiency, i.e. $T \nearrow \frac{1}{b}$ when $c \searrow 0$.

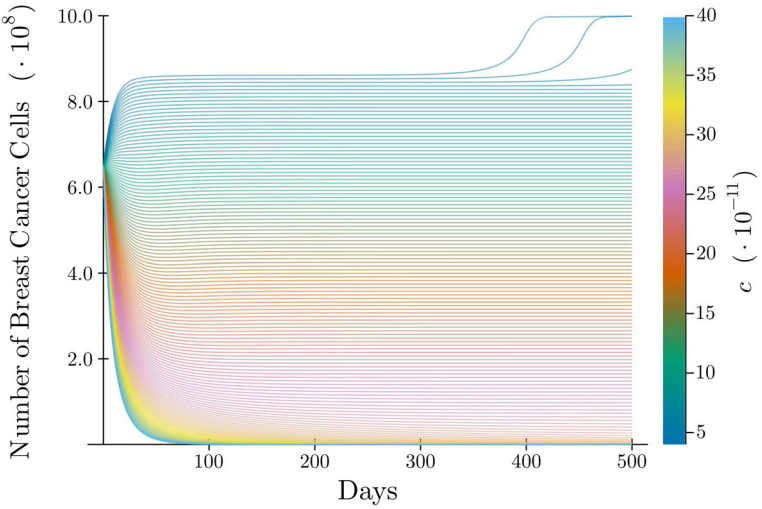

Fig. 12 Ensemble simulations of IVP, with c taking values in the 150-point discretisation of the interval $\left[4 \cdot 10^{-11}, 4 \cdot 10^{-10}\right]$ $\cdot$ cell^{-1} $\cdot$ day^{-1}, $m_T = m_T^B$, $T_0 = 6.5 \cdot 10^8$ cells, and $B_0 = 50$ cells. The phenomenon of tumour dormancy is evident, since there exist stable equilibrium points where breast-cancer-cell levels are very low (Color figure online)

5.3 Sensitivity Analysis

In this section, we perform numerical parameter sensitivity analysis in order to bring light to the dependence of the solution of our model to its parameters. Our approach is to fix all parameter values but one, which we increase and decrease by 10%, and measure the percent change of the breast cancer cell population after 200 days, when compared to the same value, but for our original parameter. We execute this procedure for four different tBregs initial conditions: $B_0 = 10^6,\ 6 \cdot 10^6,\ 11 \cdot 10^6$ and $11.5 \cdot 10^6$ cells. Additionally, we have that $T_0 = 8 \cdot 10^8$ cells, $c = 3 \cdot 10^{-10}$ cell^{-1} $\cdot$ day^{-1}, $m_T = 5 \cdot 10^{-10}$ cell^{-1} $\cdot$ day^{-1}.

The results are given in Fig. 13. In most of our experiments, the parameter showing the biggest sensitivity is, the rate at which NK cells lyse cancer cells, c. The more we increase c, the biggest the decrease in final tumour size after 200 days, further supporting Conclusion 1_a and Conclusion 1_p. Another parameter showing high sensitivity is, the tumour growth rate, a, which is to be expected. Additionally, the rest of parameters directly involving NK cells, namely, the constant source of NK cells, σ, the rate of programmable NK cell death, θ_N, and the rate of NK cell death due to Tregs, γ, all show considerable high sensitivity, which underlines the anti-tumour effect of NK cells. As far as the sensitivity of the parameters regarding Tregs is concerned, it remains almost the same, no matter the initial conditions of tBregs. On the contrary, the parameters regarding tBregs, namely, the rate of tBreg-induced Treg activation, m_B, the rate of programmable tBreg cell death, θ_B, and the rate of breast-cancer-induced tBreg activation, m_T, all show increasing sensitivity, as we increase the initial number of tBregs. This comes as a further confirmation of Conclusion 2 and Conclusion 3,

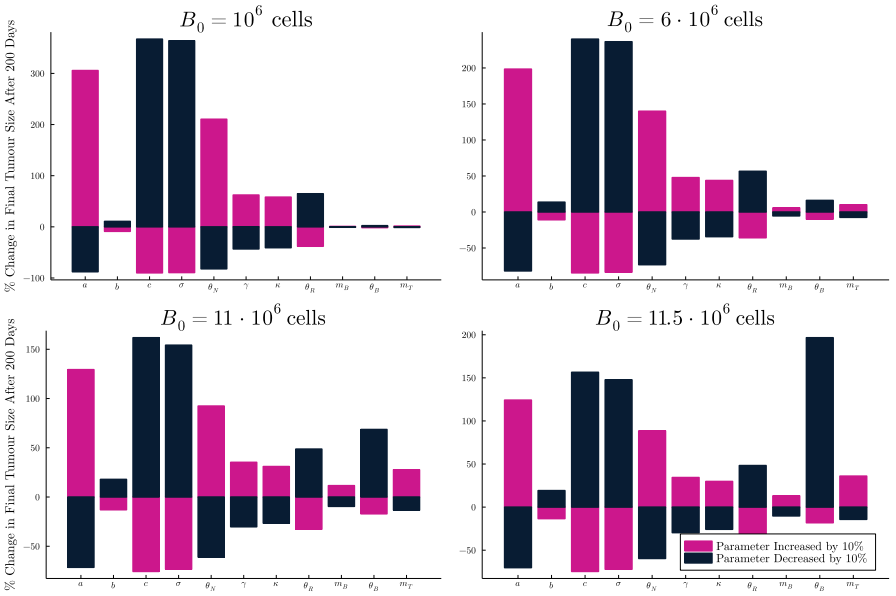

Fig. 13 Numerical sensitivity of the parameters of IVP, with $T_0 = 8 \cdot 10^8$ cells, $c = 3 \cdot 10^{-10}$ cell$^{-1} \cdot$ day^{-1}, $m_T = 5 \cdot 10^{-10}$ cell$^{-1} \cdot$ day^{-1}. The percentage change in final tumour size after 200 days is plotted. We notice that in all experiments, the parameters regarding NK cells show very high sensitivity, whereas the parameters regarding tBregs show increasing sensitivity as we increase B_0 (Color figure online)

since the higher the number of tBregs in the body, the bigger the resulting tumour, and therefore the probability of cancer metastasis is increased.

6 Conclusion and Discussion

In this study, we developed a model of non-linear ordinary differential equations, with the goal of capturing the dynamics between breast cancer cells, NK cells, Tregs and the newly discovered tBregs. An introductory approach was taken place, where the functional responses of our model were chosen to be linear (i.e. Holling's type I).

We showed the existence of three biologically realistic equilibria: an equilibrium with no cancer cells, an equilibrium with cancer cells and no tBregs, and an equilibrium with both cancer cells and tBregs. Using the linearisation and the center manifold theorem, we gave conditions regarding the local stability of each equilibrium.

Using bifurcation analysis, we showed the importance of the rate of NK-induced tumour death, c,—independently of the presence or absence of tBregs—on the stability and the existence of the equilibria, which we further proved using our numerical simulations, arriving at Conclusion 1_a and Conclusion 1_p.

Moreover, we showed how the sign of $\frac{\theta_B}{m_T} - \frac{1}{b}$ can change the number of equilibria of our model and, therefore, the dynamics of breast cancer growth. On top of that, we proved that when $\frac{\theta_B}{m_T} > \frac{1}{b}$, our model has no closed orbits, meaning that breast cancer will either be cleared by NK cells or stabilise around a constant number.

Additionally, we performed numerical simulations, in which our model was able to capture some interesting behaviours of breast cancer. On the one hand, breast cancer

cells decreased for a period of time and after reaching a minimum value, they started to increase. An opposite behaviour was also observed, with cancer cells increasing and reaching a peak, after which NK cells finally managed to clear the cancer cell population (Figs. 8 and 11). On the other hand, our model was able to capture the phenomenon of cancer dormancy, due to the existence of a stable equilibrium, in which the number of breast cancer cells is very small (Figs. 3 and 12).

Throughout our numerical simulations, the ability of tBregs to cause breast cancer cells to reach their carrying capacity was underlined, thus making us reach Conclusion 2 and Conclusion 3. In fact, our simulations showed that without tBregs, breast cancer cells can only be stabilised around two of the three equilibria admitted by our analysis (E_1 and E_2). Furthermore, even in the cases where the tumour micro-environmental conditions did not allow tBregs to grow, but only decrease—which happens when $\frac{\theta_B}{m_T} > \frac{1}{b}$—a high initial number of tBregs caused breast tumour to reach its carrying capacity. Thus, the important takeaway of this study is that when tBregs do not exist in the body, the only way for the breast tumour to reach its carrying capacity is for the rate of NK-induced breast cancer cell death to be tending to 0, whereas if tBregs exist in the body, a sufficiently large number of tBregs can cause the breast tumour to reach its carrying capacity, regardless of the rate of NK-induced breast cancer cell death. Taking all these into account, a potential tBreg-depleting therapy could minimise the ability of breast cancer to grow and metastasise.

Finally, our numerical sensitivity analysis emphasised Conclusion 2 and Conclusion 3, due to our model's high sensitivity to the parameter regarding the NK-induced death of breast cancer cells, as well as the increasing sensitivity to parameters regarding tBregs, as we increased the initial condition of tBregs.

In spite of our model's ability to be used as a framework within which we can study breast cancer growth with respect to NK cells, Tregs and tBregs, there do exist some limitations. Choosing linear functional responses has the advantage of making the model easier to approach; however, this makes our results potentially less realistic. Additionally, as tBregs are recently discovered, data regarding their kinetics do not currently exist; this drove us to estimate the value of the corresponding parameters. However, our findings could serve as a catalyst to more research regarding the function and kinetics of tBregs, which in turn could help further refine the proposed model and, therefore, the understanding of the role of tBregs in breast cancer growth and metastasis.

Acknowledgements The authors would like to thank the reviewers for their thoughtful comments and efforts towards improving the present manuscript.

Appendix

Appendix A Preliminary Results

In this section, we prove that IVP (we remind that this acronym is used for the initial value problem {(1), (2)}) has a unique solution, which is non-negative for non-negative initial conditions and for positive parameter values. We also prove that our solution

is global, i.e. it does not explode for some finite positive value of time t. The above conditions are necessary in order to assure that IVP yields biologically realistic results.

Proposition 14 (Uniqueness and non-negativity) *For every* $(T_0, N_0, R_0, B_0) \in \mathbb{R}^4_{\geq 0}$, *IVP has a unique (local) solution* $(T, N, R, B) : [0, \tau) \to \mathbb{R}^4_{\geq 0}$ *for some* $\tau > 0$.

Proof It is easy to see that the conditions of the Picard-Lindelöf theorem are fulfilled, since every function of the right-hand side of system (1) is continuous, just like its partial derivative with respect to every variable. Thus, we have that there exists a unique solution to IVP. In fact, we can extended the solution and consider it in the maximal non-negative interval of existence.

Next, we prove the non-negativity of the solution. Rewriting (1a) in the following form

$$\frac{\mathrm{d}T}{\mathrm{d}t}(t) + (cN(t) - a)T(t) = -abT^2(t)\,,$$

we notice that we have a Bernoulli equation for the variable T, and thus its solution is

$$T(t) = \frac{T_0 e^{\int_0^t (a - cN(s))\,\mathrm{d}s}}{1 + T_0 ab \int_0^t e^{\int_0^s (a - cN(\xi))\,\mathrm{d}\xi}\,\mathrm{d}s}\,,$$

which is non-negative, if T_0 is non-negative.

Using the fact that $\sigma > 0$, we turn our attention to (1b). We have that

$$\frac{\mathrm{d}N}{\mathrm{d}t}(t) > -(\gamma R(t) + \theta_N)N(t)\,,$$

and using Grönwall's inequality, we have that

$$N(t) \geq N_0 e^{-\int_0^t (\gamma R(s) + \theta_N)\,\mathrm{d}s}\,,$$

which means that $N(t) \geq 0$, when $N_0 \geq 0$.

Using a similar method as above, from (1c) we get

$$R(t) \geq R_0 e^{\int_0^t (m_B B(s) - \theta_R)\,\mathrm{d}s}\,,$$

which means that $R(t) \geq 0$, when $R_0 \geq 0$.

We then use the separation of variables method to solve (1d) for the variable B. Its solution is

$$B(t) = B_0 e^{\int_0^t (m_T T(s) - \theta_B)\,\mathrm{d}s}\,. \tag{A1}$$

Clearly, if $B_0 \geq 0$, then $B(t) \geq 0$. □

Proposition 15 *(Boundedness of T) The set* $[0, 1/b]$ *is positively invariant for the component T of the solution of IVP.*

Proof Since the solution of IVP is non-negative, we have from (1a) that

$$\frac{\mathrm{d}T}{\mathrm{d}t}(t) = \underbrace{aT(1-bT) - cNT}_{q_1(T)} \leq \underbrace{aT(1-bT)}_{q_2(T)} .$$

We assume the following two initial value problems:

$$\frac{\mathrm{d}T}{\mathrm{d}t} = q_1(T), \quad T(0) = T_0 \geq 0 \quad \text{and} \tag{A2}$$

$$\frac{\mathrm{d}z}{\mathrm{d}t} = q_2(z), \quad z(0) = \frac{1}{b} . \tag{A3}$$

Assuming that $T_0 \leq z(0) = 1/b$, and since q_1, q_2 are Lipschitz functions on $\mathbb{R}$ that satisfy the inequality $q_1(T) \leq q_2(T)$, from the comparison theorem we have that $T(t) \leq z(t)$ for t in the maximal non-negative interval of existence of the solution of IVP. Solving initial value problem (A3), yields $z = 1/b$. Hence, $T(t) \leq 1/b$, with the assumption that the initial value of T is smaller or equal to $1/b$. □

Proposition 16 *(Globality) If $T_0 \leq 1/b$, then the solution of IVP is global.*

Proof From (1d) and using the fact that $T(t) \leq 1/b$, we have that

$$\frac{\mathrm{d}B}{\mathrm{d}t}(t) \leq -\theta_B B(t) + \frac{m_T}{b} B(t) ,$$

and by using Grönwall's inequality, we have that

$$B(t) \leq B_0 e^{(\frac{m_T}{b} - \theta_B)t} .$$

Moreover, from (1c) and using the fact that $\theta_R R \geq 0$ we get

$$\frac{\mathrm{d}R}{\mathrm{d}t}(t) \leq \kappa + m_B B(t) R(t) ,$$

and by using Grönwall's inequality, we have that

$$R(t) \leq e^{m_B \int_0^t B(s)\,\mathrm{d}s} \left(R_0 + \kappa \int_0^t e^{-m_B \int_0^\xi B(s)\,\mathrm{d}s}\,\mathrm{d}\xi \right) .$$

Finally, from (1b) and using the fact that $\gamma RN \geq 0$ we get

$$\frac{\mathrm{d}N}{\mathrm{d}t}(t) \leq \sigma - \theta_N N(t) ,$$

and by using Grönwall's inequality, we have that

$$N(t) \leq \frac{\sigma}{\theta_N} - \frac{\sigma}{\theta_N} e^{-\theta_N t} + e^{-\theta_N t} N_0 .$$

Since the solution is bounded on any compact non-negative interval, we deduce its (positive) globality. □

Appendix B Parameter Estimation

Here we explain our reasoning behind our choice of parameters. Most of the parameters in our model have been chosen based on methods and data that can also be found in Bitsouni and Tsilidis (2022).

Appendix B.1 The Tumour

Based on the data fitting experiments conducted in Bitsouni and Tsilidis (2022), we chose the logistic function to model the breast cancer growth, with the tumour growth rate being $a = 0.15\ \text{day}^{-1}$ and the inverse of the tumour carrying capacity being $b = 1 \cdot 10^{-9}\ \text{cell}^{-1}$. The cell lines used for the estimation of these parameters are CN34BrM, MDA-231 and SUM1315.

Appendix B.2 The NK Cells

Healthy young adults have a total NK production rate of $(15 \pm 7.6) \cdot 10^6\ \text{cell} \cdot \text{litre}^{-1} \cdot \text{day}^{-1}$, while healthy older adults have one of $(7.3 \pm 3.7) \cdot 10^6\ \text{cells} \cdot \text{litre}^{-1} \cdot \text{day}^{-1}$ (Zhang et al. 2007). Since the average amount of blood in the human body is about 5 litre (Starr et al. 2012), the constant source of NK cells is in the range

$$\sigma \in \left[1.8 \cdot 10^7\ \text{cell} \cdot \text{day}^{-1},\ 1.13 \cdot 10^8\ \text{cell} \cdot \text{day}^{-1}\right].$$

The half-life of NK cells in humans is 1 to 2 weeks (Zhang et al. 2007) which, assuming exponential decay of NK cells, yields a range for θ_N of $(\frac{\ln 2}{14}, \frac{\ln 2}{7}) = (0.049, 0.099)$. Here, we choose an NK cells half-life of 11 days with a corresponding programmable NK death rate of

$$\theta_N = \frac{\ln 2}{11\ \text{day}} \approx 6.301 \cdot 10^{-2}\ \text{day}^{-1}.$$

Approximately 4 to 29% of circulating lymphocytes are NK cells (Keohane et al. 2015). The average number of lymphocytes per microlitre is 1000 to 4800 cells (Abbas et al. 2014), and since the average human has an average of 5 litres of blood, we have that the total population of lymphocytes in a human is $5 \cdot 10^9$ to $24 \cdot 10^9$ cells. Therefore, the total population of NK cells in blood is $N_{min} = 2 \cdot 10^8$ to $N_{max} = 6.96 \cdot 10^9$ cells. At the healthy equilibrium, our model suggests the population of NK cells to be $\frac{\sigma\theta_R}{\gamma\kappa + \theta_N\theta_R}$, which means that

$$N_{min} \leq \frac{\sigma\theta_R}{\gamma\kappa + \theta_N\theta_R} \leq N_{max} \Leftrightarrow \frac{\theta_R(\sigma - \theta_N)}{N_{max}\kappa} \leq \gamma \leq \frac{\theta_R(\sigma - \theta_N)}{N_{min}\kappa}.$$

Replacing the minimum value of σ, and the maximum value of θ_N and κ in the above inequality yields the minimum value of γ, while replacing the maximum value of

σ, and the minimum value of θ_N and κ (we derive a range for κ in Appendix B.3), yields the maximum value of γ. Finally, after calculating the above two quantities, the resulting range for the parameter γ is

$$\gamma \in \left[1.796 \cdot 10^{-12}\ \text{cell}^{-1} \cdot \text{day}^{-1}, 4.52 \cdot 10^{-9}\ \text{cell}^{-1} \cdot \text{day}^{-1}\right].$$

Appendix B.3 The Tregs

For the constant source of Tregs, our model suggests that a healthy organism has an average number of κ/θ_R Tregs, since this is the coordinate which corresponds to Tregs in the healthy equilibrium. From Pang et al. (2013) we get that Tregs are 5 to 10% of the total $CD4^+$ T cells population circulating in blood, while from Abbas et al. (2014) we get that the percentage of $CD4^+$ T cells among the total population of circulating lymphocytes ranges from 50 to 60%. Hence, the percentage of Tregs among the total population of circulating lymphocytes is 2.5 to 6%. The average number of lymphocytes per microlitre is 1000 to 4800 cells (Abbas et al. 2014), and since the average human has an average of 5 litres of blood, we have that the total population of lymphocytes in a human is $5{\cdot}10^9$ to $24{\cdot}10^9$ cells. Therefore, the total population of Tregs in blood is $1.25{\cdot}10^8$ to $1.44{\cdot}10^9$ cells. Solving the equation

$$\textit{total population of Tregs} = \frac{\kappa}{\theta_R},$$

for κ and replacing the range of values for the total population of Tregs as found above and the value of θ_R as found in the following paragraph, we finally get the constant source of Tregs to be in the interval

$$\kappa \in [4.8137 \cdot 10^6\ \text{cell} \cdot day^{-1}, 5.5454 \cdot 10^7\ \text{cell} \cdot day^{-1}].$$

The half-life of Tregs is found to be about 18 days (Mabarrack et al. 2008). Thus, assuming Tregs follow exponential decay we have that

$$\theta_R = \frac{\ln 2}{18\ \text{day}} \approx 3.851 \cdot 10^{-2}\ \text{day}^{-1}.$$

The rate of NK cell death due to Tregs, γ, is assumed to be

$$\gamma = 1 \cdot 10^{-10}\ \text{cell}^{-1} \cdot \text{day}^{-1}.$$

Appendix B.4 The tBregs

As B cells are less studied than T cells and NK cells, we are not able to find the half-life of Bregs, let alone tBregs, as they are recently discovered. So, we estimate the rate of programmable tBreg cell death to be around $\theta_B = 0.4\ \text{day}^{-1}$.

The same holds for the rate of breast-cancer-induced tBreg activation, m_T, which we assume it to be either $m_T = 5.2 \cdot 10^{-15}$ cell$^{-1} \cdot$ day^{-1} or $m_T = 5 \cdot 10^{-10}$ cell$^{-1} \cdot$ day^{-1}.

References

Abbas AK, Lichtman AH, Pillai S (2014) Cellular and molecular immunology E-book. Elsevier Health Sciences, Amsterdam

Aguirre-Ghiso JA (2007) Models, mechanisms and clinical evidence for cancer dormancy. Nat Rev Cancer 7(11):834–846. https://doi.org/10.1038/nrc2256

Al-Tuwairqi SM, Al-Johani NO, Simbawa EA (2020) Modeling dynamics of cancer virotherapy with immune response. Adv Differ Equ 1:1–26. https://doi.org/10.1186/s13662-020-02893-6

Biragyn A, Lee-Chang C, Bodogai M (2014) Generation and identification of tumor-evoked regulatory B cells. Methods Mol Biol (Clifton, NJ) 1190:271–289. https://doi.org/10.1007/978-1-4939-1161-5_19

Bitsouni V, Tsilidis V (2022) Mathematical modeling of tumor-immune system interactions: the effect of rituximab on breast cancer immune response. J Theor Biol 539, 111001. https://doi.org/10.1016/j.jtbi.2021.111001

Bray F, Ferlay J, Soerjomataram I et al (2018) Global cancer statistics 2018: GLOBOCAN estimates of incidence and mortality worldwide for 36 cancers in 185 countries. CA A Cancer J Clin 68(6):394–424. https://doi.org/10.3322/caac.21492

Bunimovich-Mendrazitsky S, Shochat E, Stone L (2007) Mathematical model of BCG immunotherapy in superficial bladder cancer. Bull Math Biol 69(6):1847–1870. https://doi.org/10.1007/s11538-007-9195-z

Byrne HM, Cox SM, Kelly C (2004) Macrophage-tumour interactions: in vivo dynamics. Discrete Contin Dyn Syst B 4(1):81. https://doi.org/10.3934/dcdsb.2004.4.81

Carol D, Rebecca S, Priti B et al (2014) Breast cancer statistics, 2013. CA A Cancer J Clin 64(1):52–62. https://doi.org/10.3322/caac.21203

Chraa D, Naim A, Olive D et al (2019) T lymphocyte subsets in cancer immunity: friends or foes. J Leukoc Biol 105(2):243–255. https://doi.org/10.1002/JLB.MR0318-097R

de Pillis LG, Radunskaya AE (2003) A mathematical model of immune response to tumor invasion. In: Computational fluid and solid mechanics 2003. Elsevier, pp 1661–1668, https://doi.org/10.1016/B978-008044046-0.50404-8

de Pillis LG, Renee Fister K, Gu W et al (2009) Mathematical model creation for cancer chemo-immunotherapy. Comput Math Methods Med 10(3):165–184. https://doi.org/10.1080/17486700802216301

de Pillis LG, Caldwell T, Sarapata E et al (2013) Mathematical modeling of regulatory T cell effects on renal cell carcinoma treatment. Discrete Contin Dyn Syst B 18:915–943. https://doi.org/10.3934/dcdsb.2013.18.915

den Breems NY, Eftimie R (2016) The re-polarisation of M2 and M1 macrophages and its role on cancer outcomes. J Theor Biol 390:23–39. https://doi.org/10.1016/j.jtbi.2015.10.034

Eftimie R, Bramson JL, Earn DJ (2011) Interactions between the immune system and cancer: a brief review of non-spatial mathematical models. Bull Math Biol 73(1):2–32. https://doi.org/10.1007/s11538-010-9526-3

Fentiman IS, Fourquet A, Hortobagyi GN (2006) Male breast cancer. The Lancet 367(9510):595–604. https://doi.org/10.1016/S0140-6736(06)68226-3

Ferlay J, Colombet M, Soerjomataram I et al (2019) Estimating the global cancer incidence and mortality in 2018: GLOBOCAN sources and methods. Int J Cancer 144(8):1941–1953. https://doi.org/10.1002/ijc.31937

Ghosh S, Banerjee S (2018) Mathematical modeling of cancer-immune system, considering the role of antibodies. Theory Biosci 137(1):67–78. https://doi.org/10.1007/s12064-018-0261-x

Gonzalez H, Hagerling C, Werb Z (2018) Roles of the immune system in cancer: from tumor initiation to metastatic progression. Genes Dev 32(19–20):1267–1284. https://doi.org/10.1101/gad.314617.118

Guo FF, Cui JW (2019) The role of tumor-infiltrating B cells in tumor immunity. J Oncol 2019:1–9. https://doi.org/10.1155/2019/2592419

He DH, Xu JX (2017) A mathematical model of pancreatic cancer with two kinds of treatments. J Biol Syst 25(01):83–104. https://doi.org/10.1142/S021833901750005X
Jordan D, Smith P, Smith P (2007) Nonlinear ordinary differential equations: an introduction for scientists and engineers. Oxford University Press, Oxford
Keohane E, Smith L, Walenga J (2015) Rodak's Hematology - E-Book: Clinical Principles and Applications. Elsevier Health Sciences, Amsterdam
Khailaie S, Bahrami F, Janahmadi M et al (2013) A mathematical model of immune activation with a unified self-nonself concept. Front Immunol 4:474. https://doi.org/10.3389/fimmu.2013.00474
Kuznetsov VA, Makalkin IA, Taylor MA et al (1994) Nonlinear dynamics of immunogenic tumors: parameter estimation and global bifurcation analysis. Bull Math Biol 56(2):295–321. https://doi.org/10.1007/BF02460644
López AG, Seoane JM, Sanjuán MA (2014) A validated mathematical model of tumor growth including tumor-host interaction, cell-mediated immune response and chemotherapy. Bull Math Biol 76(11):2884–2906. https://doi.org/10.1007/s11538-014-0037-5
Mabarrack NHE, Turner NL, Mayrhofer G (2008) Recent thymic origin, differentiation, and turnover of regulatory T cells. J Leukoc Biol 84(5):1287–1297. https://doi.org/10.1189/jlb.0308201
Makhlouf AM, El-Shennawy L, Elkaranshawy HA (2020) Mathematical modelling for the role of CD4+ T cells in tumor-immune interactions. Comput Math Methods Med. https://doi.org/10.1155/2020/7187602
Nani F, Freedman H (2000) A mathematical model of cancer treatment by immunotherapy. Math Biosci 163(2):159–199. https://doi.org/10.1016/S0025-5564(99)00058-9
Narendra BL, Reddy KE, Shantikumar S et al (2013) Immune system: a double-edged sword in cancer. Inflamm Res 62(9):823–834. https://doi.org/10.1007/s00011-013-0645-9
Olkhanud PB, Baatar D, Bodogai M et al (2009) Breast cancer lung metastasis requires expression of chemokine receptor CCR4 and regulatory T cells. Can Res 69(14):5996–6004. https://doi.org/10.1158/0008-5472.CAN-08-4619
Olkhanud PB, Damdinsuren B, Bodogai M et al (2011) Tumor-evoked regulatory B cells promote breast cancer metastasis by converting resting CD4+ T cells to T-regulatory cells. Can Res 71(10):3505–3515. https://doi.org/10.1158/0008-5472.CAN-10-4316
Pang H, Yu Q, Guo B et al (2013) Frequency of regulatory T-cells in the peripheral blood of patients with pulmonary tuberculosis from Shanxi Province, China. PLoS ONE 8(6):65496. https://doi.org/10.1371/journal.pone.0065496
Perko L (2006) Differential equations and dynamical systems, 3rd edn. Berlin, Springer
Phan TA, Tian JP (2017) The role of the innate immune system in oncolytic virotherapy. Comput Math Methods Med. https://doi.org/10.1155/2017/6587258
Rackauckas C, Nie Q (2017) Differentialequations.jl—a performant and feature-rich ecosystem for solving differential equations in Julia. J Open Res Softw 5(1):15. https://doi.org/10.5334/jors.151
Rosser EC, Mauri C (2015) Regulatory B cells: origin, phenotype, and function. Immunity 42(4):607–612. https://doi.org/10.1016/j.immuni.2015.04.005
Segel L, Cohen I (2001) Design principles for the immune system and other distributed autonomous systems. Oxford University Press, Santa Fe Institute Studies on the Sciences of Complexity
Senekal NS, Mahasa KJ, Eladdadi A et al (2021) Natural killer cells recruitment in oncolytic virotherapy: a mathematical model. Bull Math Biol 83(7):1–51. https://doi.org/10.1007/s11538-021-00903-6
Sopik V, Narod SA (2018) The relationship between tumour size, nodal status and distant metastases: on the origins of breast cancer. Breast Cancer Res Treat 170(3):647–656. https://doi.org/10.1007/s10549-018-4796-9
Starr C, Taggart R, Evers C (2012) Biology: the unity and diversity of life. Cengage Learning
Szymańska Z (2003) Analysis of immunotherapy models in the context of cancer dynamics. Int J Appl Math Comput Sci 3(13):407–418
Vaghi C, Rodallec A, Fanciullino R et al (2020) Population modeling of tumor growth curves and the reduced gompertz model improve prediction of the age of experimental tumors. PLoS Comput Biol 16(2):1–24. https://doi.org/10.1371/journal.pcbi.1007178
Villasana M, Radunskaya A (2003) A delay differential equation model for tumor growth. J Math Biol 47(3):270–294. https://doi.org/10.1007/s00285-003-0211-0
Zhang Y, Wallace DL, De Lara CM et al (2007) In vivo kinetics of human natural killer cells: the effects of ageing and acute and chronic viral infection. Immunology 121(2):258–265